Cobalt and Nickel Content in Pyrite from Gold Mineralization and Sulphide Facies Banded Iron Formation, Dickenson Mine, Red Lake, Ontario; Implication for Ore Genesis

by

Barbara Sylvia Kowalski

Submitted to the Department of Geology
in partial fulfilment of the requirements for
the degree
Bachelor of Science

McMaster University

May 1983

Bachelor of Science (1983) McMaster University

(Geology) Hamilton, Ontario

Title: Cobalt and Nickel Content in Pyrite from Gold Mineralization and Sulphide Facies Banded Iron Formation, Dickenson Mine, Red Lake, Ontario; Implication on Ore Genesis.

Author: Barbara Sylvia Kowalski

Supervisor: Dr. D.M. Shaw

Number of Pages: x, 88

To My Loving Mother

ABSTRACT

The East South C (E.S.C.) ore zone at the Dickenson Mine, Red Lake, is a major auriferous banded sulphide orebody which cross-cuts sulphide facies banded iron formation (S.F.B.I.F.) near its eastern termination. Pyrite was obtained from sulphide-rich portions of the ore zone as well as from sulphide-poor E.S.C. mineralization not spatially associated with S.F.B.I.F., S.F.BI.F., shear zone hosted mineralization such as the 1492 and F ore zones, and from quartz-carbonate vein mineralization in the South C ore zone. Forty-three pyrite separates from the zones were analyzed by Atomic Absorption Spectrophotometry for Co and Ni, in order to determine the origin of the E.S.C. ore zone. The average Ni and Co content of these pyrites are as follows: S.F.B.I.F.,7.9 and 13.6 ppm respectively; remobilized S.F.B.I.F. 10.3 and 13.6; carbonatized S.F.B.I.F. 10.9 and 22.6; South C 14.9 and 50.6; 1492 zone 34.1 and 28.4; F-zone 11.2-27.6; sulphide-poor E.S.C. 26.2 and 48.4 and sulphide-rich E.S.C., 17.91 and 16.63.

High and variable Co values were found to be associated with carbonate-rich samples, irrespective of the type of mineralization and low and similar Co values were found in all carbonate-poor samples

irrespective of their origin. Therefore, the Co content of pyrite cannot be used as a discriminant of genetically dissimilar pyrite. The Ni content in pyrite from S.F.B.I.F. is low and constant, while in shear zone and vein mineralization it is higher and more variable. The E.S.C. ore zone has similar values to that found in the epigenetic mineralization, however, a few sulphide-rich samples are similar to those found in S.F.B.I.F., suggesting a bimodal source of sulphide for the E.S.C.. It is proposed that the hydrothermal system which produced the E.S.C., 1492, F and South C ore zones, locally incorporated sulphides from the S.F.B.I.F. to produce the sulphide-rich mineralization found at the eastern extremity of the E.S.C. ore zone.

ACKNOWLEDGEMENTS

The author wishes to thank Mr. Maurice Lavigne for supplying the pyrite separates and helpful suggestions, Mr. Ota Mudroch for assisting in the laboratory, Dr. J.R. Kramer for guidance during analysis and Mr. Peter Vilks.

I express my appreciation to Dr. D.M. Shaw who supervised this research and the Department of Geology at McMaster University for the funding.

TABLE OF CONTENTS

LIST OF FIGURES

LIST OF TABLES

LIST OF PLATES

CHAPTER 1

INTRODUCTION

The East South C (E.S.C.) ore zone is a major source of gold at the Dickenson Mine, Red Lake. The mode of emplacement and temporal relationships of the ore have recently been subject to much controversy and it is the purpose of this study to bring forth evidence which may clarify its origin.

Lavigne (1983) has found many morphological and mineralogical variations of gold mineralization in the E.S.C. ore zone. The ore may occur as lenses and pods, consisting of sulphide-poor shear zones, quartz-carbonate veins and sulphide-rich impregnations. The ore zone is the on-strike continuity of the F-A-South C vein system which continues for one km to the NW, into the Campbell Red Lake Mine. The NW trending mineralization cross-cuts the E-W trending stratigraphy and at the eastern end, the E.S.C. transects an E-W trending sulphide-facies banded iron formation (S.F.B.I.F.). Here the pyrite, mineralization is sulphide-rich, and occurs as streaks of pyrite, pyrrhotite and arsenopyrite, parallel to the NW foliation in mafic volcanics altered to a quartz-muscovite-biotite-garnet-andalusite schist.

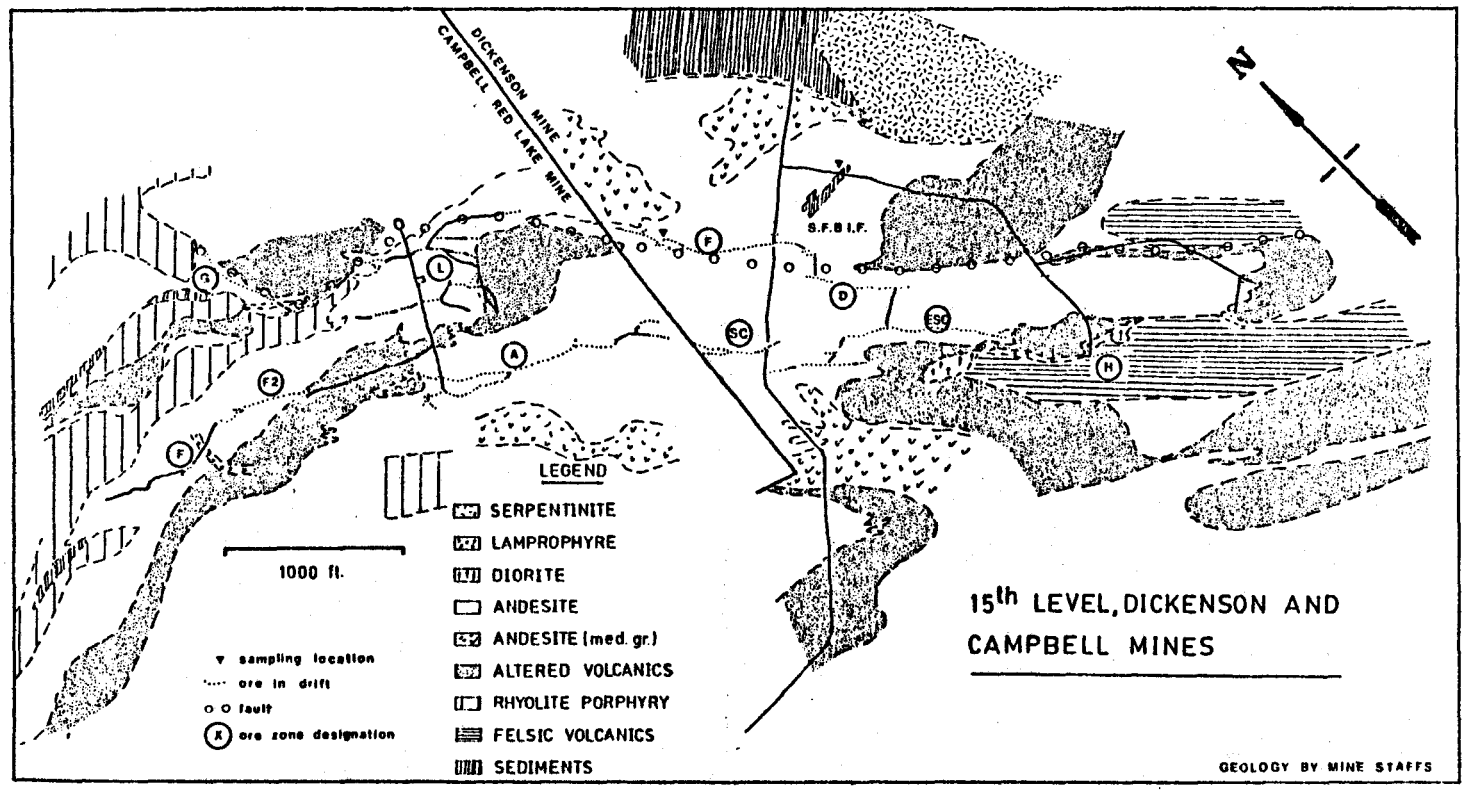
DICKENSON MINE
CAMPBELL RED LAKE MINE
N
S.F.B.I.F.
LEGEND
SERPENTINITE
LAMPROPHYRE
DIORITE
ANDESITE
ANDESITE (med. gr.)
ALTERED VOLCANICS
RHYOLITE PORPHYRY
FELSIC VOLCANICS
SEDIMENTS
1000 ft.
sampling location
ore in drift
fault
ore zone designation
15th LEVEL, DICKENSON AND CAMPBELL MINES
GEOLOGY BY MINE STAFFS

FIGURE 1-1

CHAPTER 2

OBJECTIVE

The purpose of this study is to help determine the origin of the sulphide-rich E.S.C. mineralization by analyzing the Co and Ni content of its pyrite and comparing it to pyrite whose origin is less enigmatic. Based on the close spatial association of the sulphide-rich E.S.C. mineralization and S.F.B.I.F., the following working hypothesis is proposed: Lavigne (1983) demonstrated that the sulphides in the E.S.C. were mobilized from the S.F.B.I.F. and impregnated into basalt. It is reasonable to assume that during this recrystallization in a new environment that the Co and Ni content of the pyrite will vary from that of the S.F.B.I.F.. Thus the E.S.C. pyrite will be compared to barren (sub-ore) banded sulphide impregnations in basalt which have also been demonstrated by Lavigne (1983) to have been mobilized from S.F.B.I.F.. Since the pyrite from the S.F.B.I.F. and the barren sulphides is not ore, it is necessary to make a comparison with pyrite of hydrothermal origin from ore zones that are not spatially associated with the S.F.B.I.F., such as mineralized shear zones in basalt. Quartz-carbonate vein ore will also be compared in order to determine the Co and Ni content of pyrite

which precipitated from the hydrothermal solution without being directly in contact with basalt.

In essence, the end-members are the pyrites from the hydrothermal solution and the S.F.B.I.F.. The purpose here is to use the Co and Ni content of these respective pyrites as tracers and try to identify the presence of the end-member pyrites within the E.S.C. ore zone.

As seen in Figure 2-1 the banded sulphide unit on the 27th level which impregnates basalt appears to be in complete physical continuity with deformed carbonatized S.F.B.I.F.. The purpose of determining the Co and Ni content of the pyrite from this location is two-fold: Firstly, it is the intention to check whether the carbonatized unit resembles S.F.B.I.F., and secondly, to observe the behaviour of Co and Ni pyrite upon remobilization of the sulphides and impregnation into basalt.

Pyrite was taken from the following localities:

1. E.S.C. sulphide-rich mineralization of the 30th and 24th levels;
2. S.F.B.I.F. on the 27th and 26th levels;
3. Mineralized shear zones such as the 1492 zone on the 30th level, F-zone on the 15th level, the E.S.C. ore zone on the 21st level, barren banded sulphides on the 27th level and South C quartz-carbonate ore zone on the 21st level.

All of the above are located and described in Chapter 5.

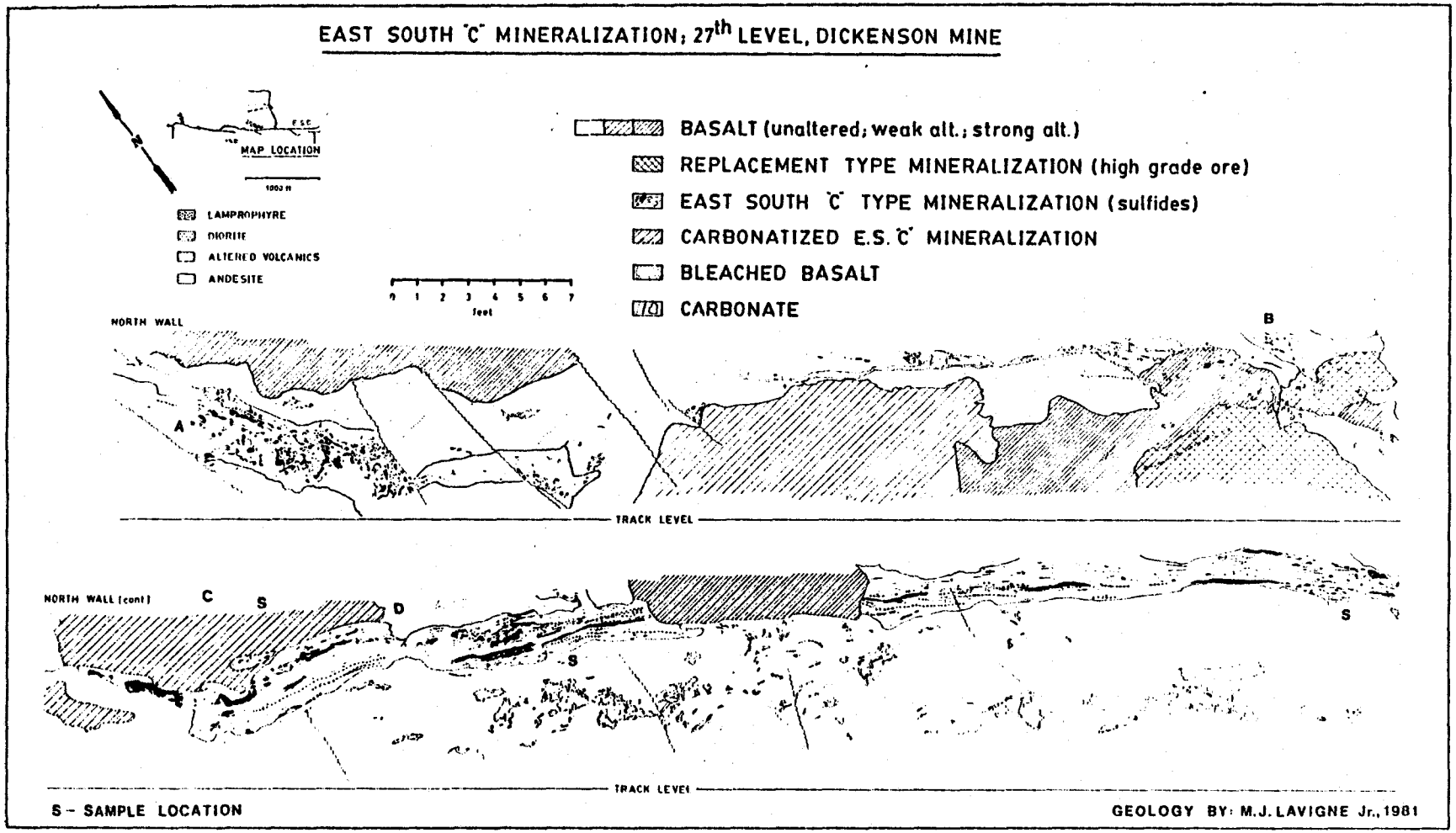
EAST SOUTH "C" MINERALIZATION; 27th LEVEL, DICKENSON MINE
MAP LOCATION
LAMPROPHYRE
DIORITE
ALTERED VOLCANICS
ANDESITE
feet
BASALT (unaltered; weak alt.; strong alt.)
REPLACEMENT TYPE MINERALIZATION (high grade ore)
EAST SOUTH "C" TYPE MINERALIZATION (sulfides)
CARBONATIZED E.S. "C" MINERALIZATION
BLEACHED BASALT
CARBONATE
NORTH WALL
A
B
TRACK LEVEL
NORTH WALL (cont)
C
S
D
S
S
TRACK LEVEL
S - SAMPLE LOCATION
GEOLOGY BY: M.J. LAVIGNE Jr., 1981

FIGURE 2-1

CHAPTER 3

GEOLOGY OF THE RED LAKE BELT

The Red Lake belt may be divided into two sequences: the lower mafic to ultramafic sequence overlain by calc-alkalic volcanics which occur in three distinct complexes. Mafic to ultramafic intrusions and felsic to intermediate subvolcanic intrusions were emplaced later in the respective complexes. The Red Lake belt was then deformed along the margins by batholiths and in the centre by the Dome Stock. The batholiths vary in composition, e.g. biotite-quartz-monzonite, hornblende-granodiorite, quartz-diorite and trondhjemites occur in the supracrustal belt. Generally, the metamorphism in the area is low-grade, except in areas that have been hydrothermally altered or near to intrusions, where it is medium-grade.

Recent dating of zircons from the felsic volcanic in the calc-alkalic complex by the U-Pb method have shown these to be younger than the lower ultramafic sequences. The ages for the northern and southern complexes are 2.70 Ma, 2.73 Ma, (H. Wallace, O.G.S., per.comm.) respectively. Dates from the felsic volcanics in the lower komatiitic-tholeiitic sequences showed ages of 2.92 Ma, 2.90 Ma, 2.96 ± 1.5 Ma and one 2.98 ± 20 Ma. (Wallace, per. comm.). Two samples taken from

the north end of McKenzie island showed zircon U-Pb ages of 2.8 Ma and 2.83 Ma.

The following descriptions were taken from Pirie (1980). The lower mafic to ultramafic flows are composed of tholeiitic basalts, tholeiitic felsic volcanics, variolitic basalts and basaltic komatiites. The tholeiitic basalts are typically medium-grained, massive, and contain pillows. Tholeiitic felsic volcanics are generally pyroclastic and occur throughout the lower mafic sequence. Variolitic basalts are pillowed and basaltic komatiites consist of " normal flows " and spinifex and polysutured flows.

Throughout the lower mafic sequence are thin interflow units of argillite, graphite argillite, chert, ferruginous chert and marble, which locally form thick sequences.

The upper calc-alkalic sequences in the Red Lake supracrustal belt are much more varied in lithology and composition than in the mafic to ultramafic sequence. Different lithologies are intimately interbedded and interdigitate laterally suggesting contemporaneous extrusion of volcanic material of different compositions. Such volcanic material includes quartz-porphyry flows, lapillistone, tuffs, rhyolitic flows and breccias intermixed with andesitic breccias, dacites, lapillistone and flows. Andesitic and basaltic flows are commonly pillowed and porphyritic.

Intense hydrothermal alteration is evident in the vicinity of the Campbell and Dickenson Mines. Where alteration is less intense

it is confined to narrow fractures filled with quartz and carbonate. In other places the altered rocks are sheared and veined but are commonly undeformed and retain pillow structures, pipe-shaped amygdules and variolitic structures.

The Red Lake supracrustal rocks have been intruded by numerous felsic to intermediate stocks and dikes, where the largest intrusive complex is the "Howey Diorite". Diabase dikes predominate in the lower mafic volcanics. Other mafic to ultramafic intrusives which occur are basaltic komatiites, serpentized peridotites and small peridotitic intrusions. These are commonly deformed to talc-carbonate-chlorite schist. The small peridotitic intrusions occur at Balmer Lake and underground at the Campbell, Dickenson and Cochenour Willans Mines. In these mines they are thoroughly altered and are referred to as "altered rock" (Campbell) and "chickenfeed" (Dickenson).

The major structure in the eastern half of the belt is a NE-trending anticline with subsidiary anticlinal and synclinal folds on both limbs. Generally, the metavolcanics and metasediments dip steeply, face NW and trend N-NE. On the south limb dips are steep, facing southward and trend eastward. No major faulting was documented in the area as outcrop is generally poor.

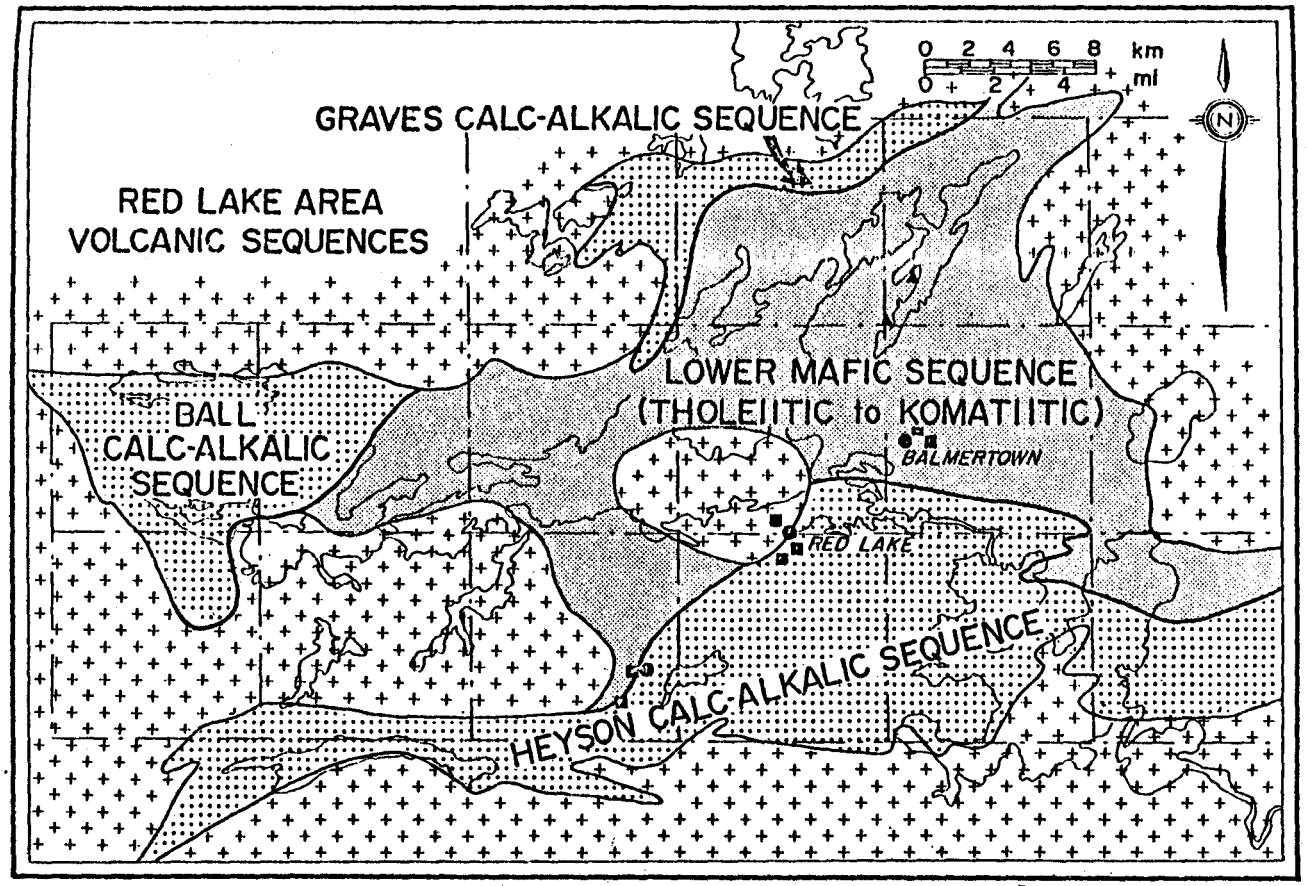

FIGURE 3-1 - Major volcanic sequences in the Red Lake area. (from Pirie, 1980)

CHAPTER 4

THE GEOLOGY OF THE CAMPBELL RED LAKE AND DICKENSON MINES

At present, the only gold producers in the Red Lake belt are the Campbell Red Lake and Dickenson mines in Balmer Township. The following descriptions and interpretations were taken directly from MacGeehan and Hodgson (1980). Pirie and Grant (1978) mapped the area on a 1:10,560 scale and follow-up detailed mapping on a 1:1200 scale was done by MacGeehan in 1978 and 1979. The mapped area may be divided into four areas: the Western Volcanic Complex (WVC), the Central Sedimentary Belt (CSB), the Eastern Volcanic Belt (EVB) and Southern Volcanic Belt (SVB). (Figure 4-1). The gold-bearing mineralized zones at the mines are located on the eastern flanks of the WVC, near its contact with the CSB.

The WVC is composed of a thick sequence of massive to pillowed mafic flows, andesites, rhyolites and minor interflow exhalative and volcaniclastic sediments which are transected by an ultramafic sill and by two thick fractionated gabbroic bodies (Campbell and Dickenson "diorites"). This complex is flanked to the east by a wedge of epiclastic conglomerates and greywackes. These rocks grade eastwards into graded wackes and mudstones which intercalate with

turbiditic exhalative sediments in the central part of the CSB. The exhalites are dominantly cherts, cherty carbonates and sulphide and oxide iron formations, and were transported into the basin by density currents from an initial depositional site higher upon the flanks of the volcanic complex. A series of mafic pillowed flows, fed through lateral feeder zones from around the periphery of the complex, intercalated with exhalative sediments along the eastern border of the CSB and thicken eastward into a major volcanic build-up (the EVB). Of particular importance is the fact that the stratigraphically equivalent rocks in the WVC and EVB were extruded during a continous period of exhalative activity and that the gold-bearing zones at the mines occur at the same stratigraphic level as exhalative sediments farther east in the CSB.

Although most of the eastern portion of the Red Lake belt has undergone greenschist facies metamorphism (Pirie, 1980), the rocks of the mines have undergone at least two stages of metamorphism: an upper amphibolite which has been overprinted by an upper greenschist metamorphism of which the latter is distinctively associated with mineralization, (Lavigne, 1983). Some of these alteration events were synvolcanic while others preceded, were contemporaneous with or post dated deformation and regional metamorphism (MacGeehan and Hodgson, 1980). Examples of alteration types include silicification, chloritization, carbonatization, spilitization and alkali-depletion. The

latter two alteration types have been recognized to be mineralogically distinct.

Spilitization is widely developed in the volcanic rocks of Balmer Township. It consists of bleached domains of Na-Si enrichment and Fe-Mg depletion which is localized around zones of primary permeability in the volcanic rocks. This alteration type occurs as bleached domains localized around quartz-epidote-carbonate-filled fissures, fractures and pipe-like circular structures in massive flows and around pillow selvages in the more permeable, pillowed flow units. The alteration is widely, but unevenly developed in the area.

Feldspar-destructive alteration is defined on the basis of the absence or low abundance of feldspar, intense Na- and variable K-depletion, and Au- and As- enrichment of the altered rocks. This alteration type is localized within and near the zone of highly fissile volcanic rocks which host the ore deposits in the Campbell and Dickenson Mines.

The dominant lithology in the Campbell Red Lake and Dickenson Mines as described by MacGeehan and Hodgson (1980) is mafic volcanic . The ore at the mines is almostexclusively hosted by this lithology. Highly altered ultramafic units are also abundant. Other minor types of lithologies are andesites, rhyolites, interflow iron formation, and volcanogenic sedimentary rocks that are transected by an ultramafic sill and by two fractionated gabbroic bodies (Campbell and Dickenson 'diorites'). Most of the rocks have undergone deformation

and are highly foliated compared to the lithologically similar rocks away from the mines. The amount of strain and the degree of fissility of the rocks depends in part on lithology. The ores are hosted by a narrow highly fissile zone. At the mines the pillowed basalt and andesites are more strongly foliated and schistose, whereas, the interflow sedimentary rocks are commonly intensely deformed and internally folded. The mafic and intermediate pillowed flow-units face south in both mines. The gabbroic and ultramafic intrusions are not as foliated and deformed as the other lithotypes of the mines.

The mineralization described by Hodgson, Helmstaedt, MacGeehan and Rigg (1979-80) occurs as three types: 1. Fissure filling veins of banded carbonate (dolomitic), 'chert' (very fine-grained quartz), arsenopyrite- quartz, pyrite, magnetite, and native gold. 2. Silicified replacement mineralization in which both the rock and pre-existing fissure veins were replaced by fine-grained granulose quartz, auriferous arsenopyrite, pyrite and native gold. 3. Disseminated banded sulphide mineralization in silicified volcanic rocks and iron formation occur in the East South C ore zone of the Dickenson Mine which is in strike continuation of the F-A-South C fissure vein system in the Campbell and Dickeson Mine.

The geology of the E.S.C., F and South C ore zones will be discussed in further detail in the following chapter.

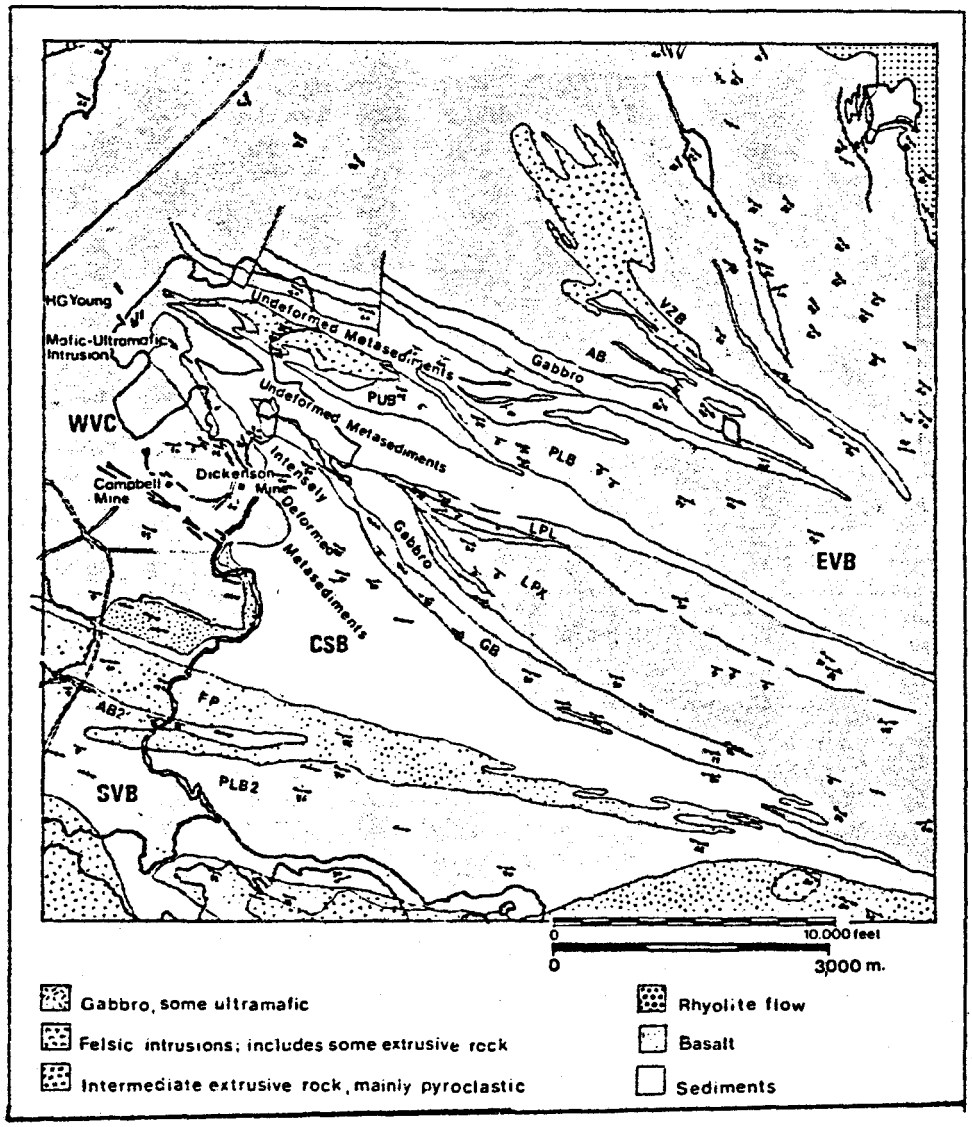

FIGURE 4-1 Geology of the western part of Balmer Township. (from Hodgson et al., 1980, modified after MacGeehan and Hodgson, 1980)

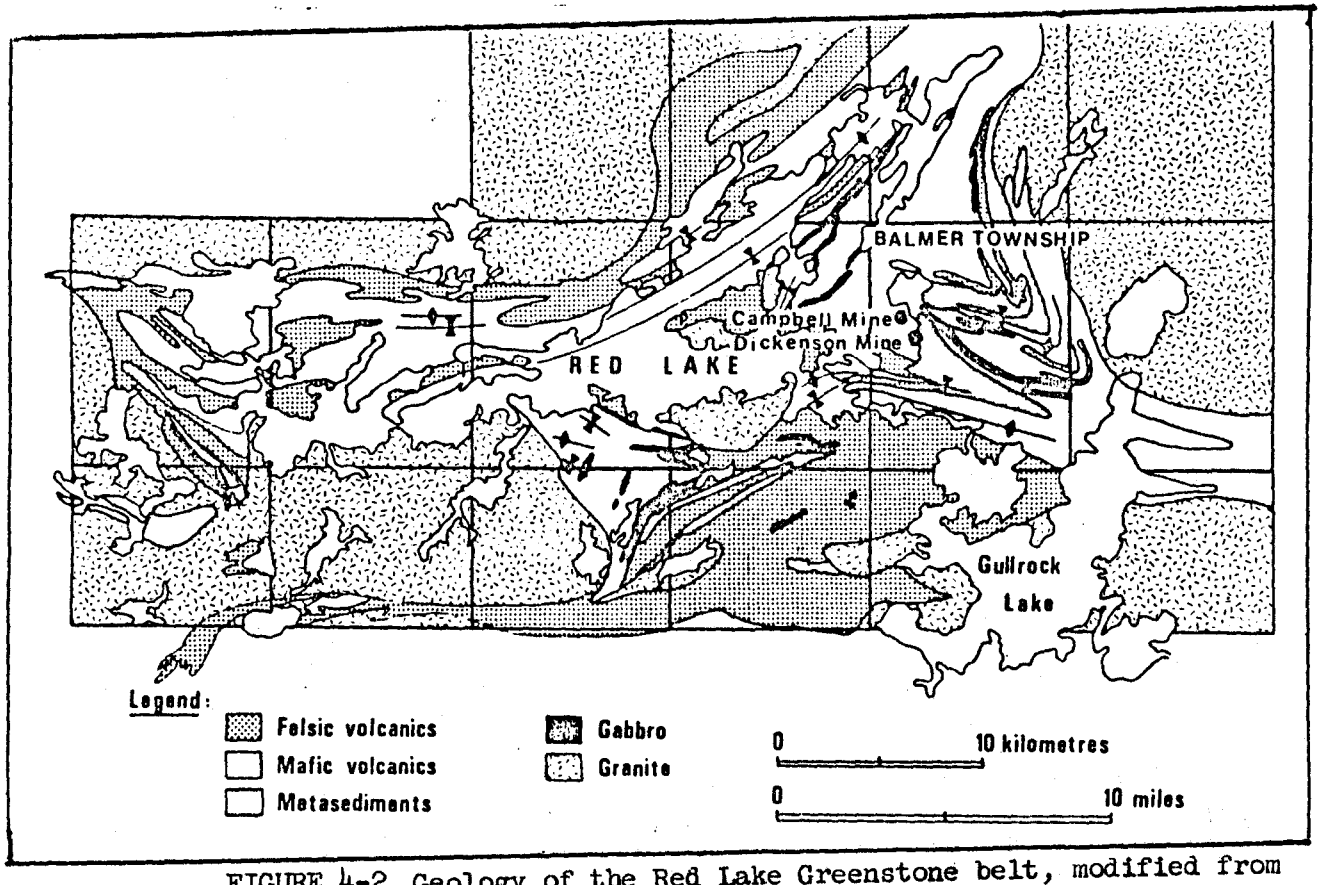

FIGURE 4-2 Geology of the Red Lake Greenstone belt, modified from the O.G.S. Geological Compilation Map 2175.

CHAPTER 5

DESCRIPTIONS OF SAMPLE LOCATIONS

The purpose of this chapter is to describe the geology and mineralogy of the localities in which the pyrite samples were taken. Petrographic description of the mineralogy coexisting with pyrite enables one to study the effects that the mineralogy may have on the Co-Ni content of pyrite. Table 5-1 is a summary of the detailed petrographic descriptions presented below. The carbonate content of all the samples available was determined by point counting and the results are summarized in Table 5-1. The purpose of carbonate analysis is seen in Figure 8-1, where a correlation between carbonate and Co exists. The modal percentages of the sulphides and oxides used here were taken from Lavigne (1983).

5.1 BARREN BANDED SULPHIDE, 27TH LEVEL

Lavigne (1983) describes sub-ore E.S.C.-type mineralization on the 27th level. Figure 2-1 is a detailed map of the northwall of the drift. Graphitic S.F.B.I.F. is intersected by the drift forty feet to the NW of the western limit of this map. The S.F.B.I.F. trends

E-W, unlike the E.S.C.-type mineralization which trends NW, parallel to the foliation and the drift. The preservation and exposure of this same S.F.B.I.F. is much better on the 26th level (175' directly above) than on the 27th level.

The most westerly sulphide-rich exposure at points A and B in Figure 2-1 consists of streaky sulphides, parallel to foliation and has a fragmental appearance due to abundant zones of contorted, folded banded sulphides, consisting of deformed S.F.B.I.F.. Point C represents a unit which consists of carbonatized S.F.B.I.F.. From point D onwards to the southeast, Lavigne (1983) demonstrates that the sulphides impregnate basalt and are probably a remobilizate from the S.F.B.I.F., as the ore is in complete physical continuity with the S.F.B.I.F.. This unit is typical E.S.C. mineralization, however, it is not ore. Thus at this location there is an opportunity to examine not only the Co- Ni content of pyrite from the S.F.B.I.F. but also to examine the changes of Co-Ni content of pyrite remobilized from S.F.B.I.F. and impregnating into the basalt. Although the sulphide impregnations in the basalt resemble typical E.S.C. mineralization that are not ore and have the same Au content as the iron formation, the Co-Ni contents may represent remobilized iron formations without the superimposed effects of ore-bearing fluid (Figure 8-1).

Samples ML-81-062 and ML-81-051 are altered volcanic rocks. Polished thin section examination of these samples show disseminated fine (less than 1mm) to medium-grained pyrite as defining less than

0.5cm bands. This pyrite is set in quartz and biotite, whereas, in the carbonate-rich parts of the rock they occur as coarse-grained sulphides, and pyrite is uncommon. Ilmenite occurs in small laths oriented parallel to the foliation. Pyrrhotite is a minor phase which forms pseudomorphs after pyrite, which retain the cubic shape. Arsenopyrite occurs as specks throughout the gangue. Ilmenite, arsenopyrite and magnetite are all minor phases. (Plates 5-1,5-2,5-3).

The rocks consist of fine-grained quartz, carbonate, plagioclase (oligoclase), andalusite, biotite and muscovite. The latter three define a weak foliation. These sections are homogeneous throughout, with respect to the mineral assemblage present.

Examination of hand specimen from the S.F.B.I.F. on the 26th levels reveals this iron formation to be variably deformed, consisting of folded 0.2 to 0.1 cm pyrite bands and lesser pyrrhotite, interbanded with black siliceous graphitic bands and cherty quartz.

5.2 24TH AND 21ST LEVELS EAST SOUTH C

The ore lens from the E.S.C. zone on the 21st level, in the 21-12102 stope is 80ft. in length and 7ft. in width (Figure 5-1). Lavigne (1983) described it as a linear, foliation parallel shear zone in pillowed amygdaloidal basalt, the pillow and amygdules being preserved in areas of low strain within the ore. This ore lens is sulphide-poor,

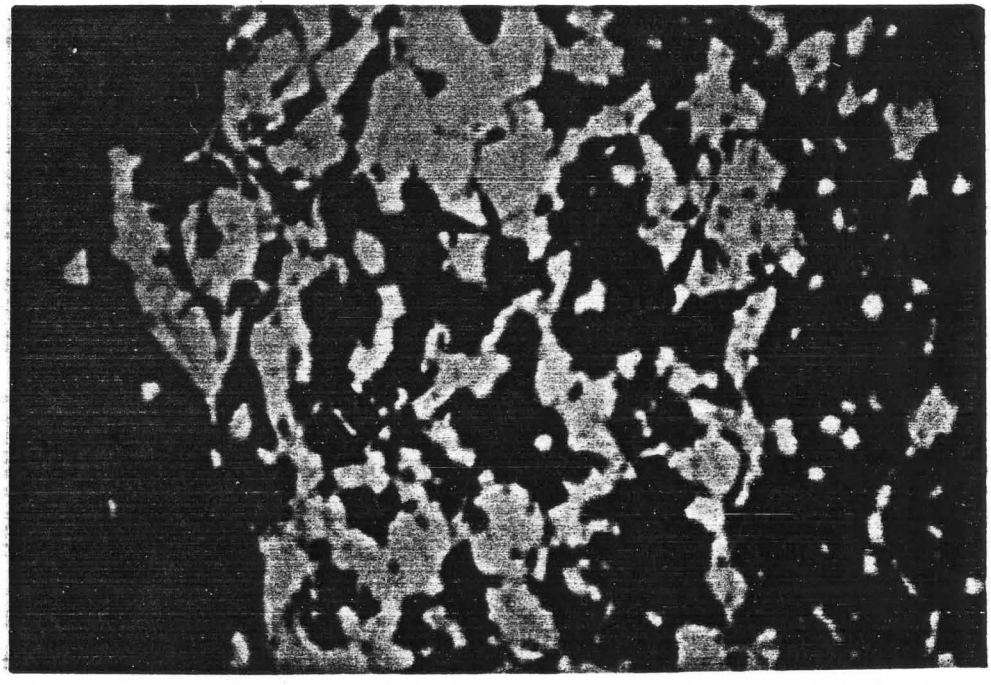

PLATE 5-1. Banded pyrite set in quartz and biotite.
Sample ML-81-062

PLATE 5-2. Disseminated pyrite in sample ML-80-051.

PLATE 5-3. Same as Plate 5-2. Pyrite is surrounded predominately by carbonate. Quartz and andalusite are present.

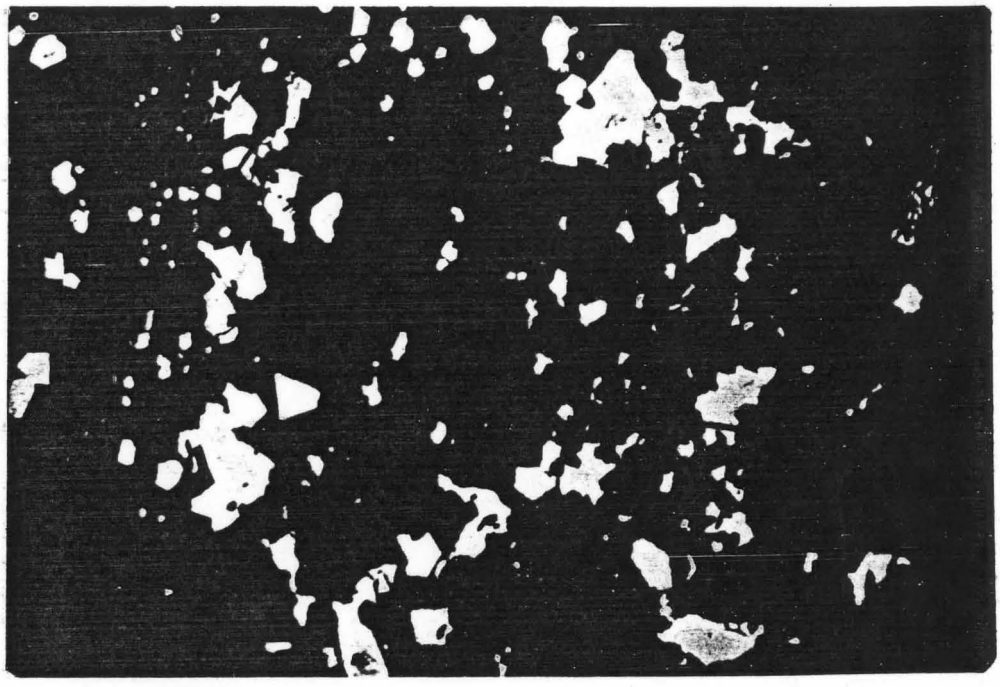

1mm

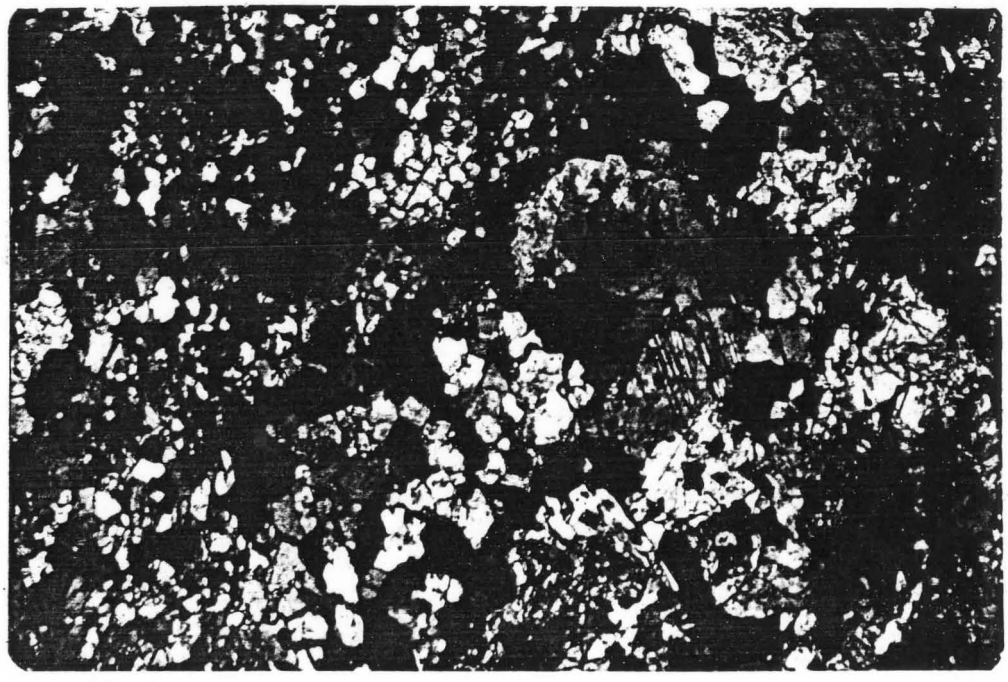

1mm

unlike sulphide-rich E.S.C. mineralization associated with S.F.B.I.F.. Section ML-80-953 has 1.5% pyrite, 3.3% pyrrhotite, 1.1% arsenopyrite and 0.4% magnetite while section ML-80-956 has 0.2% pyrite, 1.6% pyrrhotite, 3.6% arsenopyrite and 0.8% magnetite, all of which are finely disseminated (Plate 5-4). The ore zone is a well foliated quartz-biotite- carbonate- muscovite- andalusite schist, muscovite being more abundant in areas of higher strain which also have an associated grain size decrease.

Sulphide-rich E.S.C. mineralization is found at the eastern termination of the 24th level (Figure 5-2). Lavigne (1983) has recognized two types of mineralization in this area. One consists of a siliceous fragmental rock with sulphides in the matrix and the other a massive pod of siliceous arsenopyrite-rich high grade ore.

The fragmental ore is interpreted by Lavigne(1983) as a highly deformed S.F.B.I.F.. Sample ML-80-939 taken from this location consist of 7.0% pyrite occurring as streaks, 3.7% disseminated arsenopyrite rhombs and 2.2% pyrrhotite which occur irreguarly. Sample ML-80-939 consists of quartz, biotite, muscovite, carbonate plus other minor phases. This section is mineralogically variable with respect to the proportion of silicates from one part of the section to the next. A muscovite slip area divides domains of variable mineralogy. This section is strongly foliated. Brecciation, also appears in this section and may have been caused by a later foliation cross-cutting an earlier foliation. Thus the sulphides, silicates and carbonates

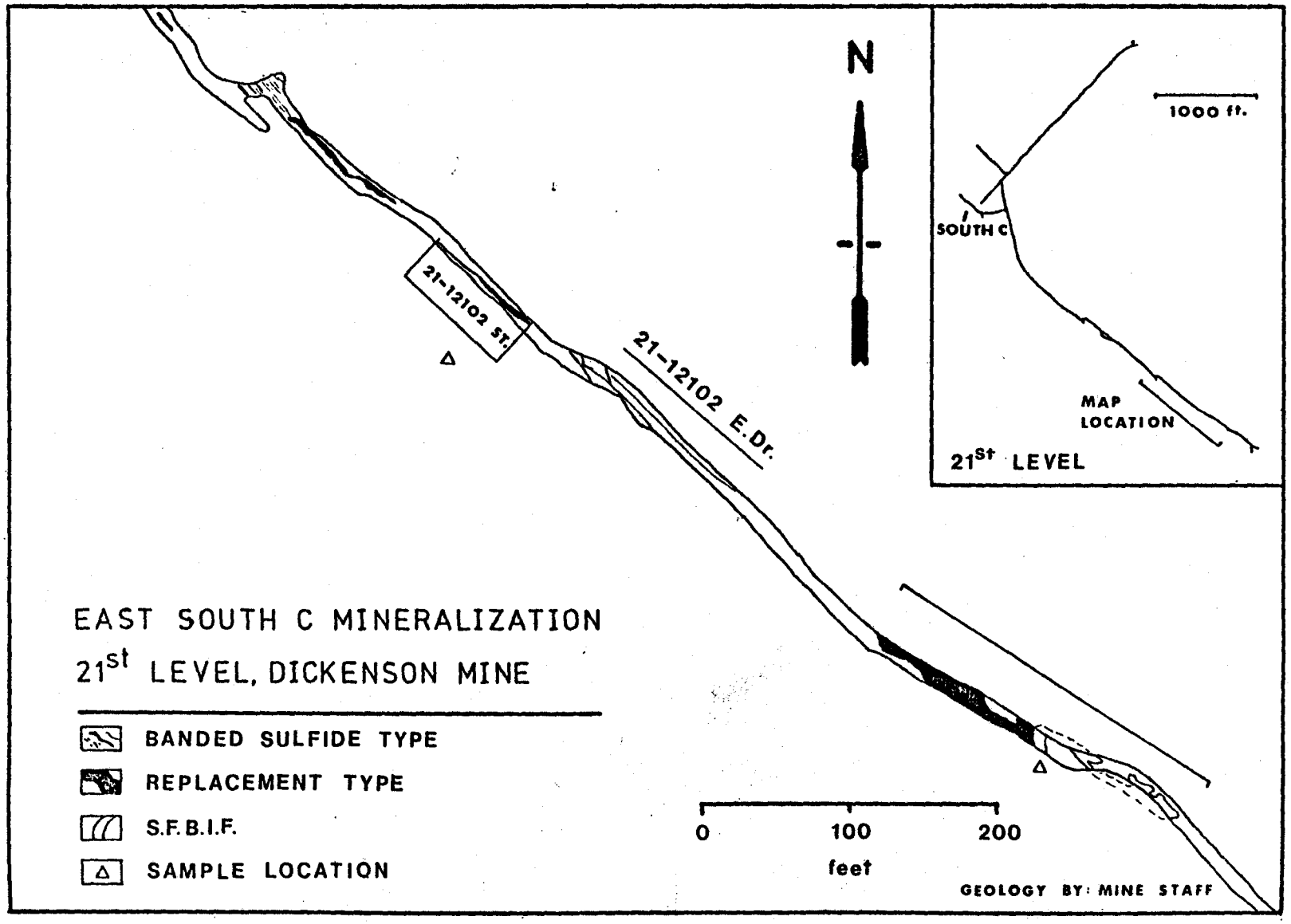
N
1000 ft.
SOUTH C
MAP LOCATION
21ST LEVEL
21-12102 ST.
21-12102 E.Dr.
EAST SOUTH C MINERALIZATION
21st LEVEL, DICKENSON MINE
BANDED SULFIDE TYPE
REPLACEMENT TYPE
S.F.B.I.F.
SAMPLE LOCATION
0
100
200
feet
GEOLOGY BY: MINE STAFF

FIGURE 5-1

present during the first foliation have been further broken into smaller grain sizes during the second foliation.

Sample ML-80-042 taken from a silicified pod of mineralization has 13.9% arsenopyrite and 3.0% pyrite. Magnetite (0.4%) occurs as a minor phase. Section ML-80-043 is made up of the same sulphides and oxides as in -042, but in addition it has porphyroblasts of pyrrhotite grains that are highly fractured. In places the pyrrhotite completely encloses euhedral pyrite grains. The modal percents of pyrite, pyrrhotite, arsenopyrite, magnetite are 1.7, 6.5, 14.0, 0.9, respectively. Sample ML-80-042 (Plate 5-5) is a strongly foliated muscovite-biotite schist. Muscovite defines the fabric along with the elongated quartz grains. Biotite is absent in those highly strained areas. Occasionally, relics of andalusite and staurolite are preserved locally. In areas of low to medium strain, relics of plagioclase, andalusite, garnet porphyroblasts and staurolite are present along with tourmaline, dumortierite and green biotite. Section ML-80-043 is similar in textures and in mineralogy as above. An additional feature seen is arsenopyrite replacing plagioclase.

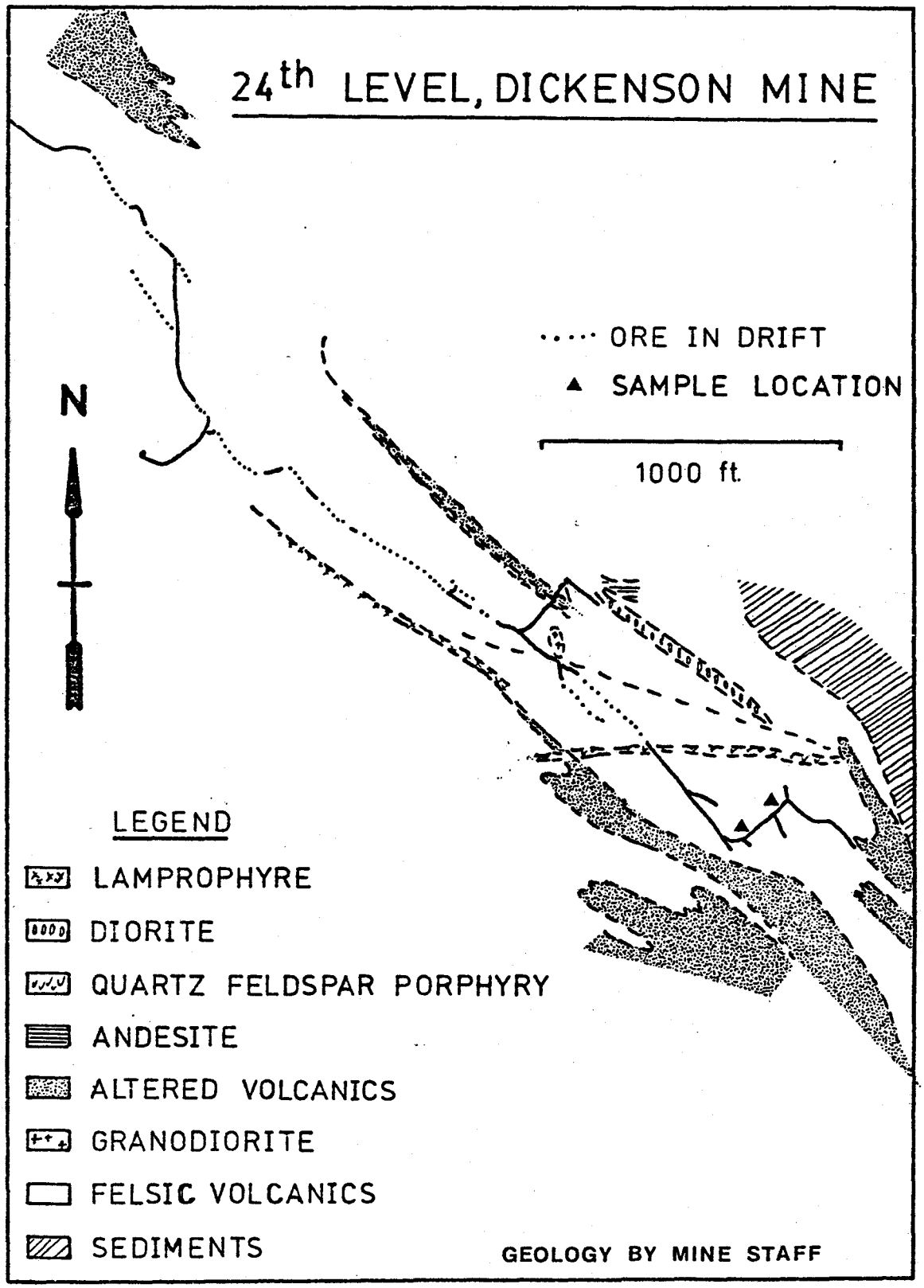
24th LEVEL, DICKENSON MINE
ORE IN DRIFT
SAMPLE LOCATION
1000 ft.
N
LEGEND
LAMPROPHYRE
DIORITE
QUARTZ FELDSPAR PORPHYRY
ANDESITE
ALTERED VOLCANICS
GRANODIORITE
FELSIC VOLCANICS
SEDIMENTS
GEOLOGY BY MINE STAFF

FIGURE 5-2

PLATE 5-4. Disseminated pyrite, pyrrhotite, arsenopyrite, in sample ML-81-955 from E.S.C. ore on 21-12102 stope.

PLATE 5-5. Arsenopyrite (smaller grains and aggregates) and pyrite (large subhedral, scratched grain) from arsenopyrite replacement type mineralization; magnetite is dark grey; sample ML-80-042.

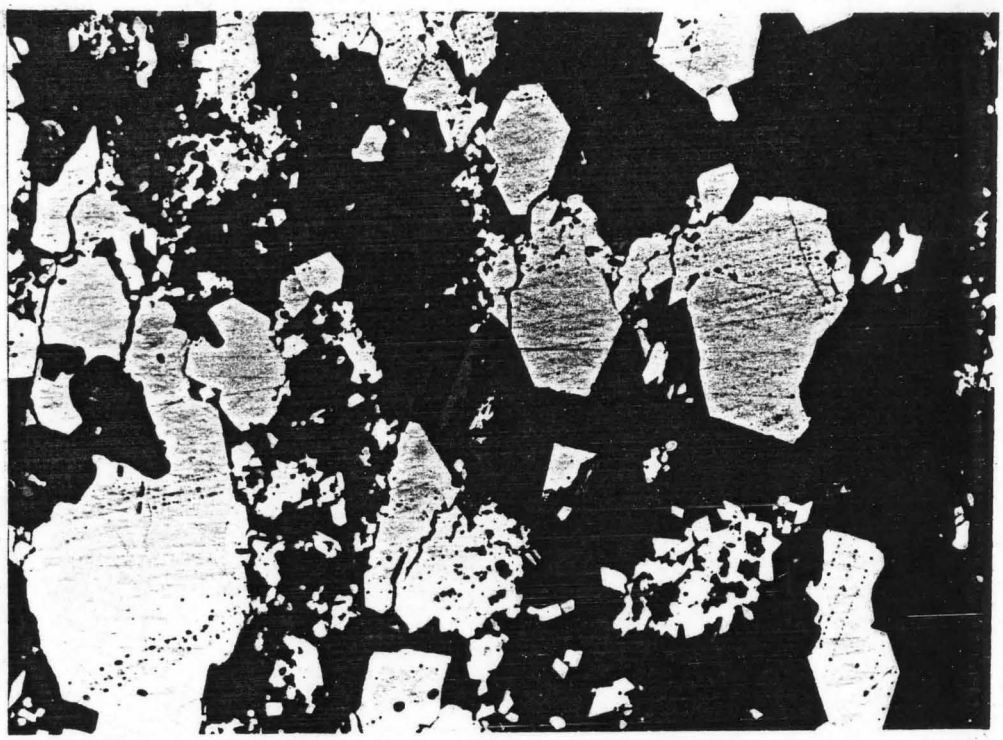

1mm

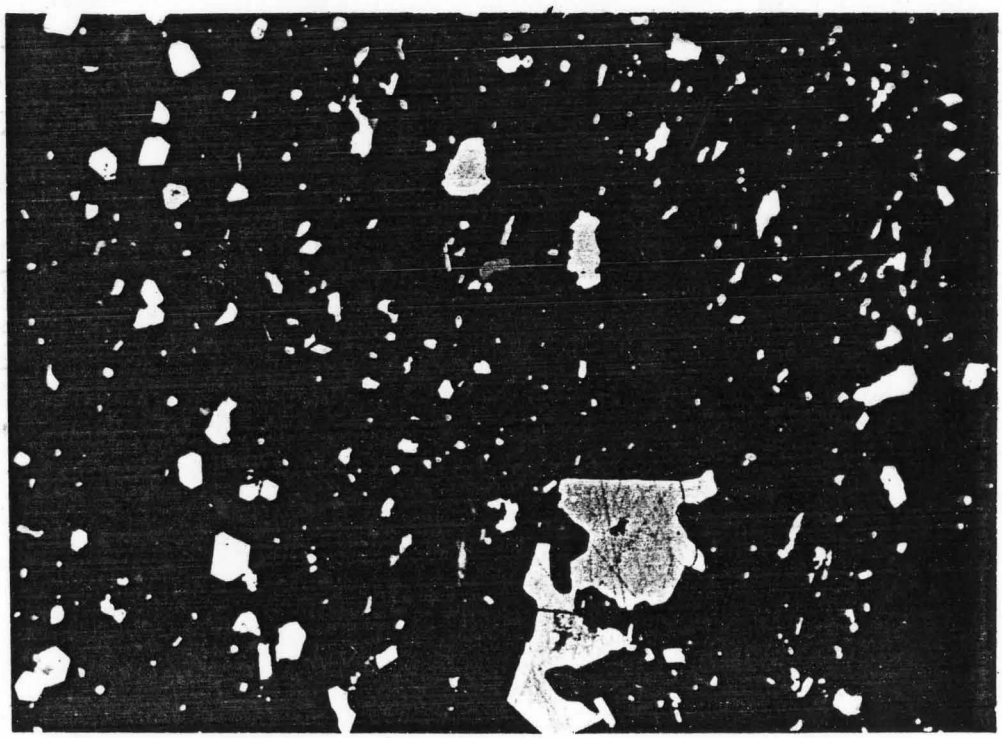

1mm

5.3 30TH LEVEL Δ3053 SAMPLES ML-80-618, -870 to -873 Δ3058 SAMPLES -605, -611

This area described by Lavigne (1983) is a typical E.S.C. sulphide-rich zone. The sulphides have impregnated a well banded, foliated garnetiferous mafic volcanic wallrock. It is spatially asscciated with the S.F.B.I.F. and sample locations are shown in Figure 5-3.

The sulphides in section ML-80-618 are mainly pyrrhotite (5.0%) and minor pyrite. Magnetite occurs as a minor phase (0.9%). Section ML-80-870 is predominantly made up of disseminated pyrite (8.7%). Larger grains show signs of cataclasis. The pyrite in this section is generally irregular in form and smaller grains appear rounded. Other sulphides in this section are pyrrhotite (o.4%), and arsenopyrite (o.4%). Magnetite occurs as a minor phase (0.2%).

Pyrite in section ML-80-871 occurs as a minor phase, (3.7%) and is fine-grained. Arsenopyrite sometimes occurs in streaks and follows the strong foliation. Arsenopyrite (6.8%) occurs in irregular, framboidal-like crystals. It is seen replacing pyrite. There is 0.2% magnetite in this section. (Plate 5-6).

Pyrite (13.9%) in section ML-80-872 is medium- to coarse-grained and shows signs of cataclasis. Occasionally, large allotriomorphic pyrite crystals are wrapped by pyrrhotite (5.2%). Pyrrhotite shows signs of deformation such as subgraining and crenulated granulation.

Pyrite (13.2%) in section ML-80-873 is the dominant sulphide. In some areas of the section pyrite is allotriomorphic, other areas it is disseminated and shows signs of cataclasis. Occasionally, euhedral pyrite grains are wrapped by pyrrhotite. Pyrrhotite (5.4%) shows subgraining. Magnetite (0.9%) occurs as a minor phase. The foliation in this section is strong.

Pyrite in section ML-80-605 is disseminated and coarse grains show pronounced cataclastic textures. The pyrite constitutes 16.1% of the section. Ilmenite occurs as a minor phase.

Pyrite in section ML-80-611a occurs as a massive vein. It shows mild signs of cataclasis. Pyrite constitutes 32.4% of the section. It shows subgraining and has been literally shredded in places. It constitutes 0.9% of the section. Magnetite and ilmenite occur as minor phases.

Mineralogically, ML-80-618 is banded. The bands are made up of sulphides, quartz, biotite, andalusite, plagioclase and minor amounts of carbonate. Plagioclase (oligoclase), hornblende crystals and garnet porphyroblasts are local. Quartz and carbonate occur as lenses and are seen locally.

ML-80-870 is very fine-grained and weakly foliated. The primary mineral is quartz which is typically elongated and parallel to the foliation and occasional porphyroblasts occur. Biotite and muscovite are also very fine-grained.

Section ML-80-871 is essentially the same as -870 but the carbonate content is lower.

The principal minerals in section ML-80-872 are garnet, quartz, biotite, carbonate, muscovite and plagioclase. Garnets are seen to be stretched and are overgrown by idiomorphic grains of pyrite that have no fabric. Fine-grained sulphides which have been stretched and bent; elongated quartz grains and fine-grained muscovite define a foliation. These fine-grained minerals wrap other rounded garnet porphyroblasts. Plagioclase is seen to have overgrown sulphides. In areas of high strain associated minerals are muscovite and elongated quartz grains.

In moderately strained areas small scale kinking of sulphides, muscovite and quartz are seen. In areas of low strain relic textures of garnet, plagioclase, quartz, relic foliations and biotite are noted.

Section ML-80-873 is made up of a few thin 0.5cm bands. One band is made up of sulphides, pargasite and cummingtonite. There is some andalusite and garnets are highly corroded and are occasionally seen in part being replaced by biotite. Garnets have crystallized to form garnetifierous bands that are parallel to the foliation. Muscovite, biotite, quartz and pargasite are observed to have overgrown garnets. There is no carbonate in this section.

Section ML-80-605 has several pyrite bands which are in contact predominantly with quartz grains. Other minerals are muscovite and dumortierite which are very fine-grained, but the latter also occasionally appears as porphyroblasts. This section is moderately foliated.

Section ML-80-611a is predominately composed of quartz, biotite, plagioclase, andalusite, which are associated with the sulphides. Locally, hornblende relics are preserved.

5.4 F-ZONE 15TH LEVEL

F-zone (Figure 1-1) described by Lavigne (1983) is similar to the E.S.C. on the 21st level and the 1492 zone (described later). It is essentially a sulphide-poor shear zone within mafic volcanics.

The pyrite in section ML-80-986 (Plate 5-7) is medium-grained and is the predominant sulphide. It is disseminated and occurs in streaks. Idiomorphic pyrite grains are occasionally seen to be

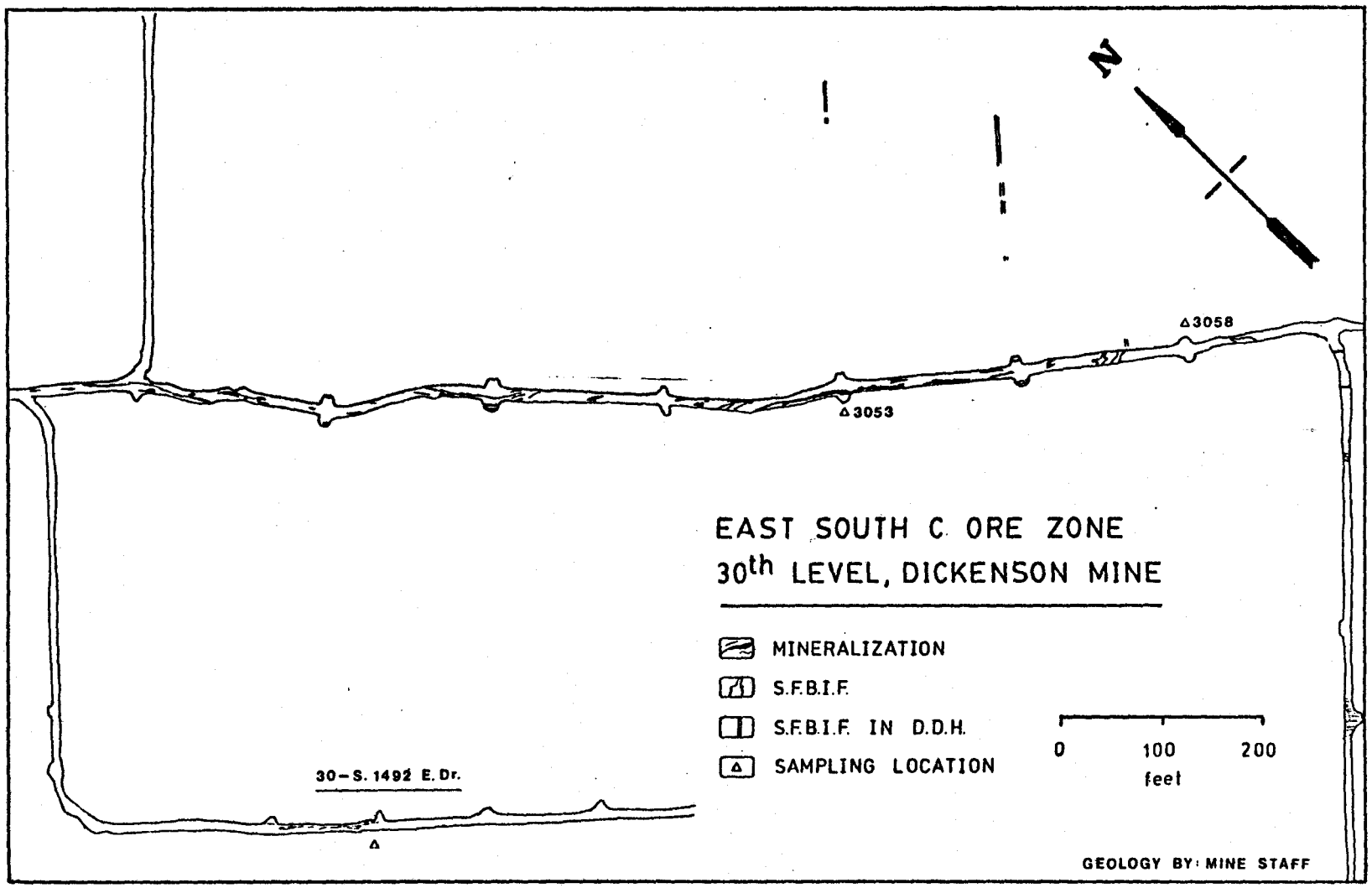
N
Δ3058
Δ3053
EAST SOUTH C ORE ZONE
30th LEVEL, DICKENSON MINE
MINERALIZATION
S.F.B.I.F.
S.F.B.I.F. IN D.D.H.
SAMPLING LOCATION
0
100
200
feet
30-S. 1492 E. Dr.
GEOLOGY BY: MINE STAFF

FIGURE 5-3.

PLATE 5-6. Arsenopyrite (white) and pyrite (light grey), note arsenopyrite replacing pyrite. Sample ML-80-871 E.S.C. ore zone 30th level.

PLATE 5-7. Disseminated pyrite and pyrrhotite in sample ML-80-986 from the F-zone 15th level.

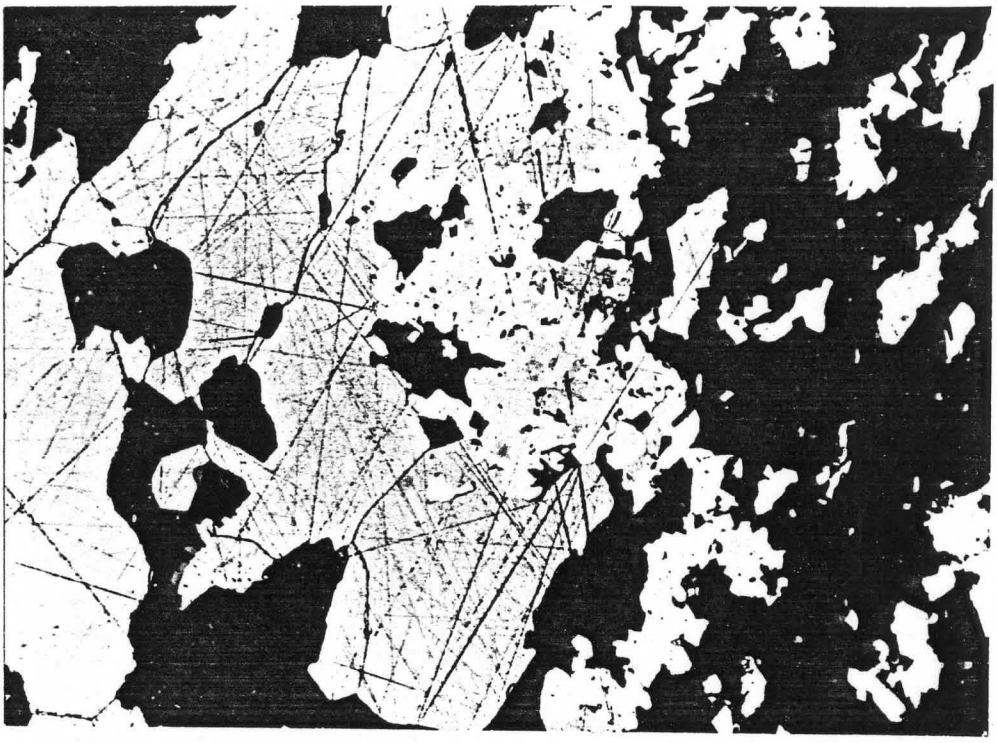

1mm

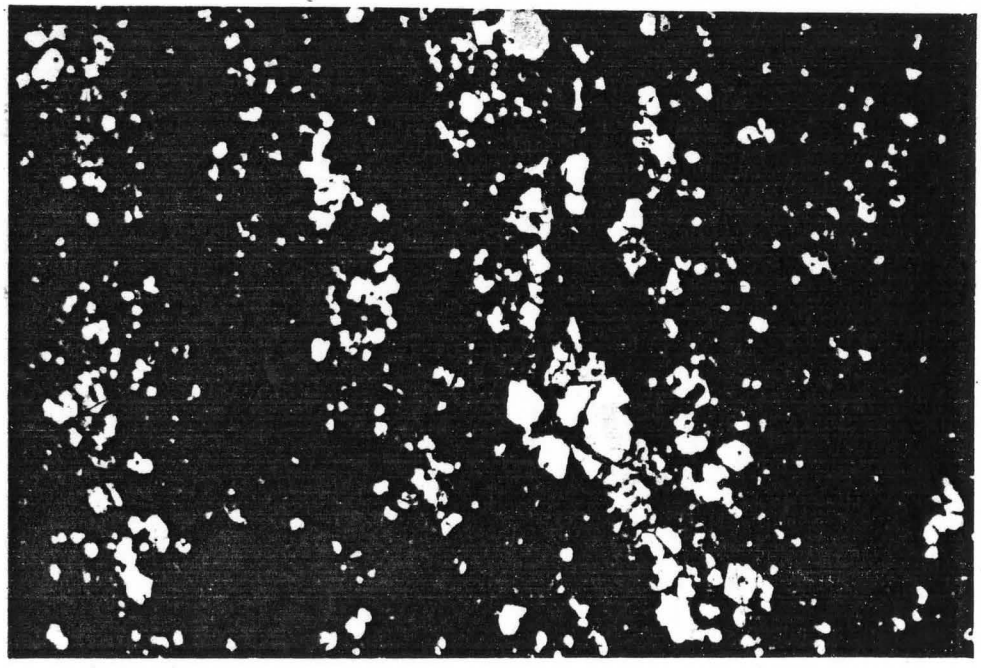

1mm

enclosed by pyrrhotite. Pyrrhotite is allotriomorphic and is sub-grained. Sulphides are common within boudins of andalusite. Boud-inaged quartz veinlets are present where the biotite and muscovite define each boudin. This section is moderately foliated and small scale kinking is seen. Dumorterite has also been observed.

5.5 1492 ZONE 30TH LEVEL

The 1492 zone described by Lavigne (1983) is a sulphide-enriched shear zone in pillowed amygdaloidal basalt. The ore lens (Figure 5-3) is 200' in length and 8' wide. This ore lens is similar to the 21st level E.S.C. described earlier.

Thin sections for the samples analysed were not available. Lavigne (1983) described other thin sections from this area (Plate 5-8). The sulphides are disseminated throughout the sections. Pyrrhotite, magnetite, and ilmenite predominate. Arsenopyrite forms rhombs that make up a band and are seen replacing pyrrhotite.

Mineralogically, the 1492 zone is generally a quartz-biotite-muscovite schist. The sulphides are generally associated with these minerals.

5.6 SOUTH C 21ST LEVEL

The South C ore zone shown in Figures 1-1 and 5-1, represents a typical carbonate and cherty quartz fissure filling vein. Lavigne (1983) describes this area in further detail.

The pyrite in section ML-80-126 is allotriomorphic. It is a minor phase and is seen to be enclosed by pyrrhotite (Plate 5-9). Pyrrhotite is also allotriomorphic, and is the predominating sulphide. Ilmenite occurs throguout the section as small laths oriented preferentially to the weak foliation. This section shows part of a carbonate-quartz vein, in which the sulphides are associated with carbonate. Other minerals in the sample include cummingtonite, biotite, muscovite, plagioclase and hornblende.

PLATE 5-8. Disseminated pyrite, pyrrhotite, arsenopyrite and magnetite in sample ML-80-553 from 1492 zone, Dickenson Mine.

PLATE 5-9. Pyrrhotite with minor pyrite from the South C 21st level, Dickenson Mine.

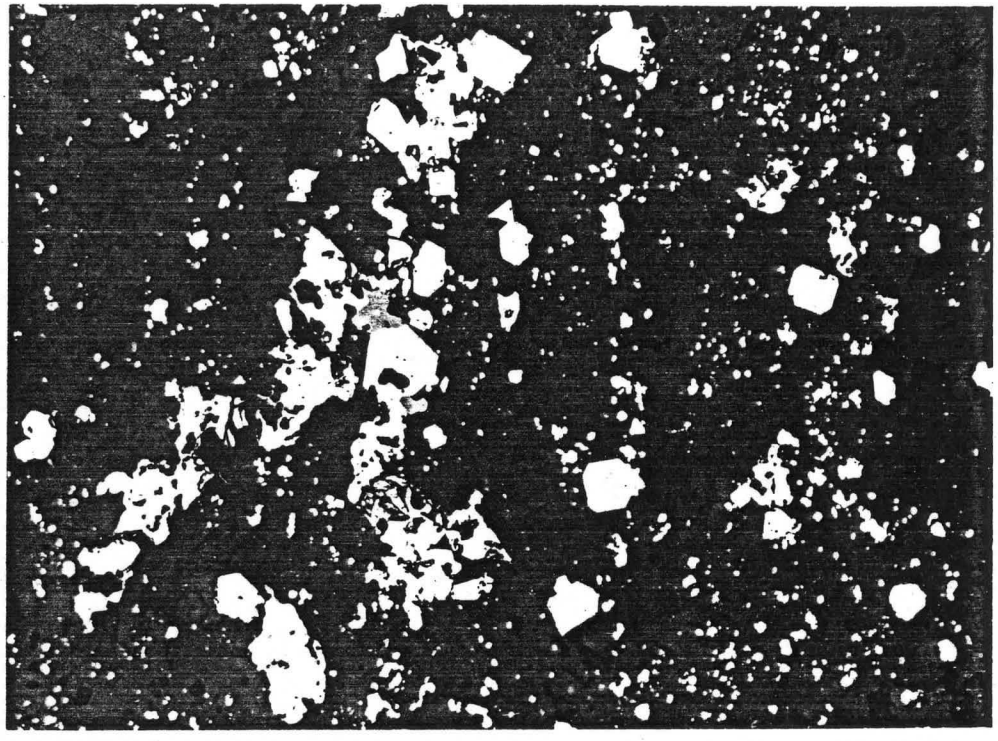

1mm

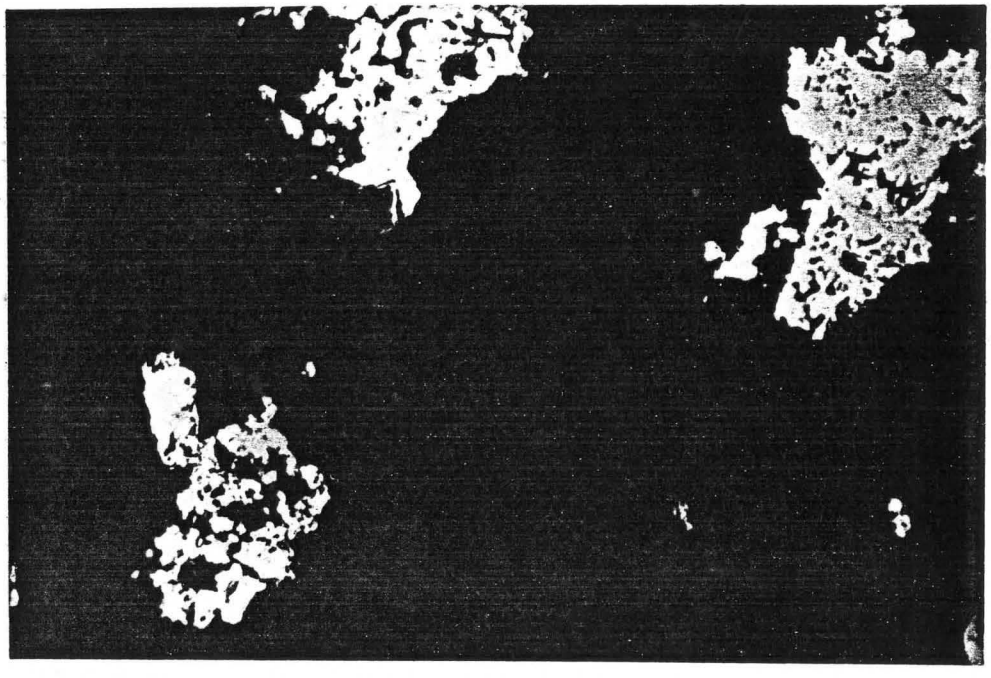

1mm

Table 5 -1 Summary of Petrographic Descriptions

Location	Sample #	Co (ppm)	Ni (ppm)	Polished Thin Section	Thin Section	%Carbonate
Banded Sul. 27th L.	ML-81-062	14.68633	11.09628	-py,po,apy,ilm,mgt	-qtz,carb,olig,andal, biot,musc.	8.55
Banded Carb. Sul. 27th L.	ML-81-051	21.48352	15.82892	-py,po,apy,ilm,mgt	-qtz,carb,olig,andal, biot,musc.	12.83
Carbonated S.F.B.I.F. 27th Level- no sections available						
26th Level S.F.B.I.F. - no sections available						
21st L. E.S.C.	ML-80-953	26.43487	28.15875	-py,po,apy,mgt	-qtz,carb,olig,andal, biot,musc.	17.0
	ML-80-954	59.93350	23.39474	-py,po,apy,mgt	-qtz,carb,biot,musc.	21.65
	ML-80-956	58.99045	27.02937	-py,po,apy,mgt	-qtz,czrb,andal,biot, musc.	
24th L. E.S.C.	ML-80-939	14.95450	12.62619	-py,po,apy	-qtz,carb,biot,musc.	3.42
	ML-80-942	13.16385	18.32342	-py,apy,mgt	-qtz,carb,olig,andal, staur,gt,tour,dum.	1.71
	ML-80-943	16.31484	18.59260	-py,po,apy,mgt	-qtz,carb,olig,andal, staur,gt,tour,dum.	7.41
E.S.C. 30th L.	ML-80-618	15.79318	18.38037	-po,mgt	-qtz,carb,olig,andal, biot,hnbe,gt.	9.11
	ML-80-870	14.19759	21.15396	-py,po,apy,mgt	-qtz,carb,biot,musc.	5.12
	ML-80-871	9.78645	27.31096	-py,apy,mgt	-qtz,carb,biot,musc.	4.27
	ML-80-872	15.28757	12.92161	-py,po	-qtz,carb,olig,biot, musc,gt.	1.42

Table 5-1 continued

Location	Sample #	Co (ppm)	Ni (ppm)	Polished Thin Section	Thin Section	%Carbonate
E.S.C. 30th L.	ML-80-873	13.72107	12.00908	-py,po,mgt	-qtz,andal,biot,musc, gt,parag,cummingt.	0
	ML-80-605	16.06900	17.98842	-py,ilm	-qtz,musc,dum.	0
	ML-80-611	10.32901	15.45841	-py vein,po,ilm,mgt	-qtz,carb,olig,biot, hnbe	2.27
F-zone 15th L.	ML-80-986	10.10046	12.54109	-py,po	-qtz,carb,andal,biot, musc,dum.	0.2
1492 zone 30th L.	--	--	--	-py,po,apy,ilm,mgt	-qtz,carb,musc,biot.	22.58
South C 21st L.	ML-81-126	10.12710	17.84643	-py,po,ilm	-qtz-carb vein,olig, musc,biot,hnbe	6.8

CHAPTER 6

PYRITE CRYSTAL CHEMISTRY

It is the purpose here to discuss the reasons why certain elements will occur in sufficient concentrations in pyrite and be useful indicators of the physical-chemical conditions of crystallization. The following material was taken directly from Burns (1970), Hulliger (1968), Price (1972), Nickel (1968), Bither et. al. (1968) and Ryall (1979).

The pyrite structure is a face-centred array of cubic close-packed ions with NaCl-type structure. The formula AX_2 denotes A as a transition-element cation and X as a chalcogen or pnigogen anion. The most common cations involved are Co, Ni, Fe, Mn and Cu while less common cations are Ti, V, Cr, Zn, Au, Ag. Common anions are the chalcogen elements S, Se, Te and the pnigogen elements As, Sb, Bi. (Hulliger, 1968). According to Burns (1970) the crystal field theory describes the origins and results of the surroundings (electrostatic fields) on the orbital-energy levels of a transition metal. A transition element is one which has a partly filled 3d or 3f shell such as Ti, V, Cr, Mn, Co, Ni, Cu, An and Fe. At specific orbital energies, that is, at low energy orbitals,

transition-metal ions stabilize and are incorporated into the pyrite lattice. Overlap of the transition-metal (cation) orbitals and certain orbitals of anions (ligands) such as sulphides and arsenides leads to bond formation. The different relative enrichments of Co over Ni in pyrite and pyrrhotite respectively, may be explained by the occurrence of low-energy orbitals and high-energy orbitals respectively in the two sulphide phases. (Point counting results of pyrite and pyrrhotite listed in chapter 5 compared with results of Co and Ni obtained, (Tables 8-2,8-3) could not verify this preferential acceptance of Ni and Co in pyrite and pyrrhotite). The stabilization energy, resulting from bond formation in compounds with acceptor ligands lead to enrichments of certain transition-metal ions. The preferential acceptance of one transition element over another in the pyrite lattice is also due to chemical nature of the medium from which pyrite crystallizes, that is, pH, Eh, temperature, activity of vapour phases. To crystallize pyrite from a fluid which carries certain minor elements the conditions the pyrite must form under are low Eh, low $pS^{=}$, pH 7.37 and a reducing environment, (Berner , 1971). According to Bezmen et. al. (1975) the temperatures at which the pyrites used in this study crystallized at, were determined to be greater than 500 C. This is discussed in Chapter 8.

Finally, it is important to understand the possible means by which minor elements are incorporated onto pyrite. They are the following (Ryall, 1979):

1. surface adsorption;
2. occlusion-impurities trapped by growth of the host crystal;
3. solid-solution where the trace element substitutes for an atom in the host crystal;
4. exsolution-separation of phases on cooling;
5. concentration in structural defects (discontinuities, grain boundaries, incipient cleavage planes, etc.).

The following chapter discusses the method by which Co and Ni values were obtained.

CHAPTER 7

METHOD OF ANALYSIS

7.1 SAMPLE PREPARATION

Pyrite separates were provided to the author by M. Lavigne. Samples ML-80-872 and ML-80-081 were analyzed by XRD to determine whether marcasite was present. The results showed only pyrite. Most of the separates were prepared by the acid digestion method described by Lavigne (1983), but a few were impure due to separation by a hydraulic method described by Lavigne (1983). These latter samples were finely-ground with a mortar and pestle. Polished thin section examination revealed that the pyrite is inclusion free.

The separates were purified by the acid digestion method as follows. Each powdered sample was put into a teflon crucible, wetted with distilled water and treated with approximately 20ml of hydrofluoric acid (50% strength) and 20ml of hydrochloric acid (37% strength). The crucibles were covered and left in a hot bath for 48 hours, following which they were treated with 40ml of boric acid (5% strength).

Following this treatment, they were drained and washed thoroughly with acetone (99.5% strength), leaving most of the sulphides without any silicate. In some cases, however, a residue was still

present and the sulphides plus impurites were transferred onto an hour glass. The impurities were lightly disaggregated by hand and then washed away with acetone. This procedure was repeated until greater than 99 per cent purity was achieved. Then the samples were left to dry, and were examined under the binocular microscope and all visible impurities were removed with tweezers.

Solutions were made from the pyrite for Atomic Absorption Acetylene Flame Spectrophotometry. The procedure is described in detail in Figure 7-1. The solutions were then analyzed for cobalt and nickel. Following the analysis, six pyrite solutions were noticed to have residual silicates. The solution was filtered through the Nudepose paper to remove residual silicates which were then weighed. Those six samples with maximum residues are compared in Table 7-5. It can be seen from this table that the percent particulates left in the solution is not significant and should not affect the analytical results. Most other samples underwent complete dissolution.

7.2 ATOMIC ABSORPTION ACETYLENE FLAME SPECTROHOTOMETRY

Samples were analyzed on a Perkin-Elmer 603 Atomic Absorption Acetylene Flame Spectrohotometer according to the procedures outlined by Perkin Elmer (1976). The spectrophotometer operates with an air/acetylene flame, at a temperature of 2145 C. (Reeves and Brooks, 1978). The flame oxidizes a lean blue colour

The following method was taken from Maxwell (1968) p.439

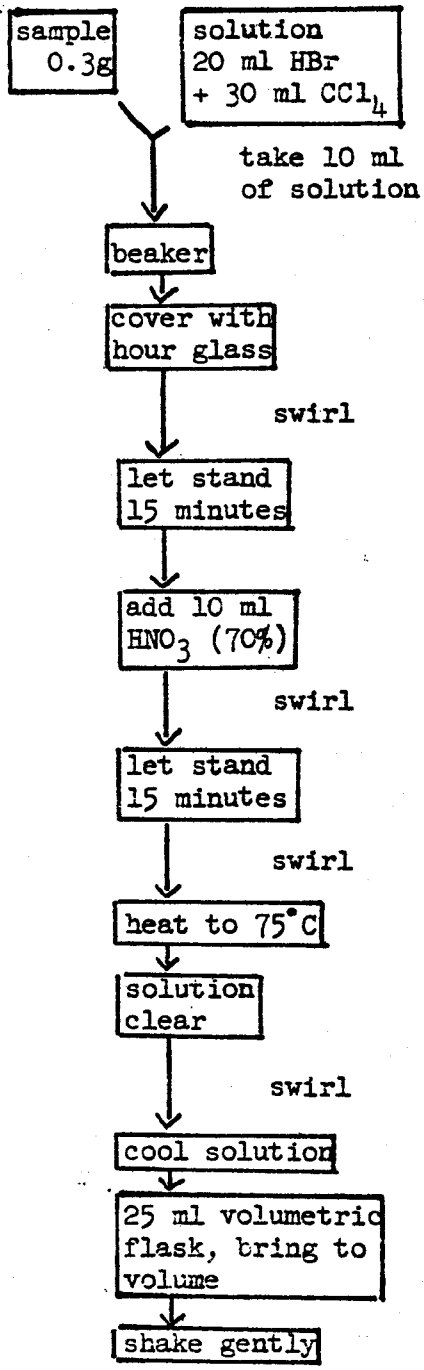

NOTE: pH of most of the solutions prepared was determined to be 0.2.

FIGURE 7-1 Preparation of pyrite solutions.

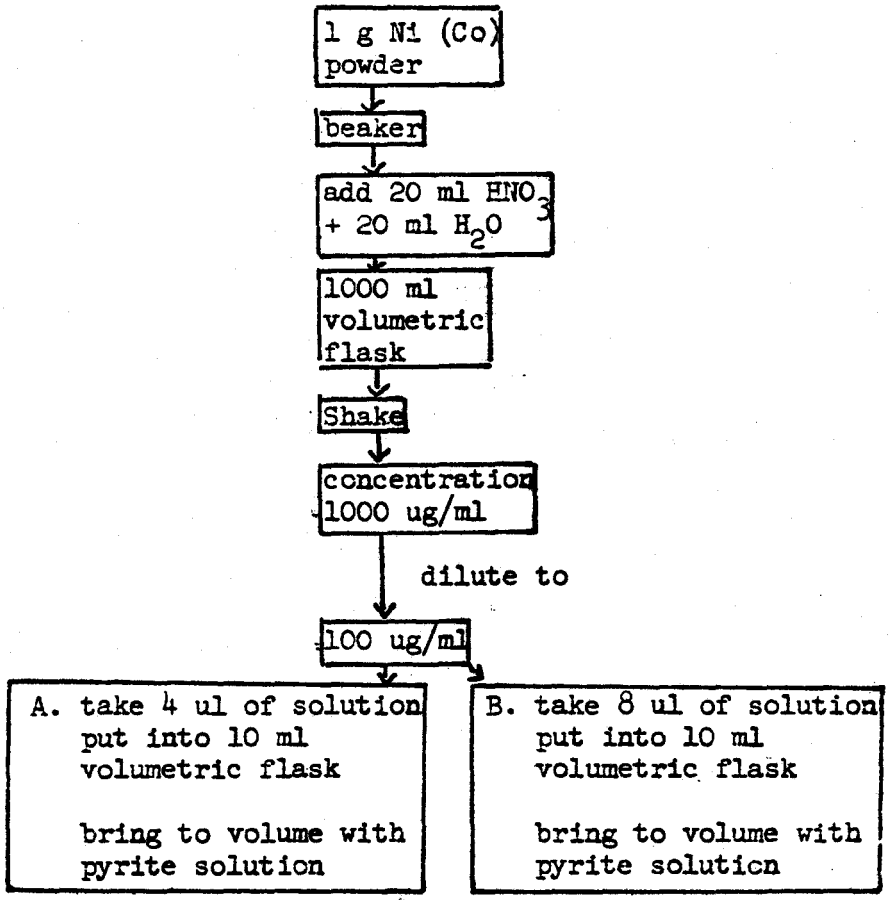

- see Appendix for calculations

FIGURE 7-2 Preparation for Ni and Co spiking solutions

for Co and Ni. A multiple hollow cathode lamp with Co and Ni elements was used. The lamp current was set for 30 mA. The wavelength used for Ni and Co were 232.0 nm and 240.7 nm respectively. The UV range was set for 0.7 nm.

During analysis of pyrite, matrix interference problems can be controlled by having standards with the same composition as the analyte. The most precise method is to use each sample as its own standard. Thus the background absorbances are always equal in the sample and standards. This can be achieved with the standard additions method, as follows:

The sample solution is divided into three aliquots. A known increasing amount of Co and Ni solution is added to all but one aliquot to be determined. The solutions are then brought up to the same volume. Then the absorbance can be interpreted as follows: The working curve shown in Figure 7-3 passes through the three analytical points and intersects the concentration axes. An analogous curve, shown by the dashed line, is parallel to the solid line but passes through the origin. The line must be linear (if it is curved then errors have been introduced), and may be represented by $y=mx+b$. By using this linear function and by similar triangles the concentration, represented by the point C_o, required may be determined.

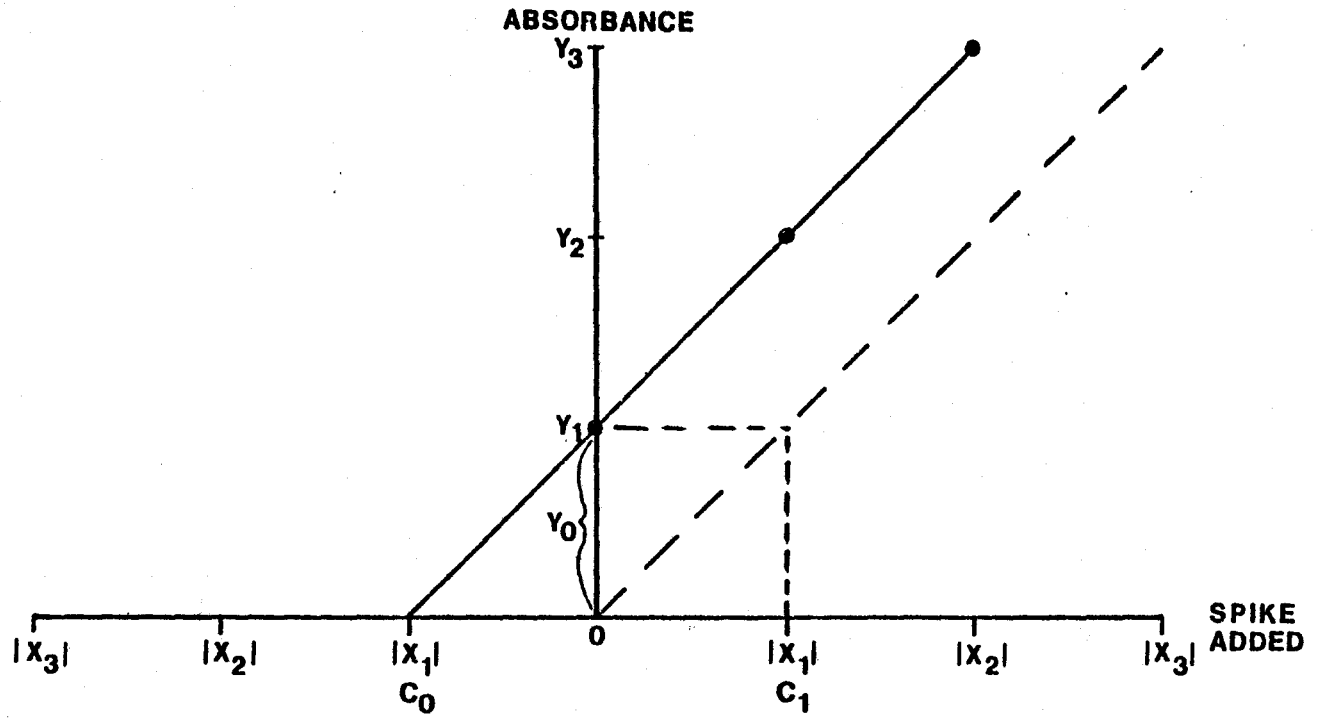

FIGURE 7-3. Standard Additions Method.
Y_1 = absorbance of unspiked solutions + background absorbance and scatter.
Y_2 = absorbance of unspike solution + background absorbance and scatter + x ug/l metals added.
Y_3 = absorbance of unspiked solution + background absorbance and scatter + 2x ug/l metals added.

7-3 PRECISION

The samples available varied in weight. Those which were much less than 0.1g in size were analysed and were found to be at the detection limit of the spectrophotometer, thus they were not plotted in Figure 8-1. All other samples available weighed between 0.1g and 0.3g. Thus it is important to determine whether the precision depends on sample weight.

Sample number ML-81-123 was divided into four-0.3 g samples (ML-81-123 A, B, C, D) and four-0.1 g samples (ML-81-123 E, F, G, H). These samples were analysed and reanalysed several weeks later and the results are shown in Table 7-1 (i). Referring to Figure 8-1, it is seen that the cobalt clusters into two distinct groups at 0.1g and 0.3g samples. The nickel results do not vary to the extent of the cobalt data. This discrepancy within the cobalt data may be explained by an interference effect (discussed later). All steps leading to sample and sample solution preparation were done identically. Thus the difference seen in the cobalt analysis could not have been the the result of error during or prior to sample solution preparation, since one would expect a similar error to occur in the nickel data. Therefore, the problem was will be attempted to be shown later is an interference effect from within the atomic absorption spectrophotometer.

7.4 ACCURACY

Accuracy of the analysis cannot be determined since an external standard with a similar matrix to pyrite is not available.

7.5 INTERFERENCES

It is the purpose of this section to determine the types of interference that could have affected the cobalt results. Thus the interferences will be listed and the applicable possibilities will be noted.

7.5.1 Sample Introduction

The accuracy and precision of the signal response may be affected by the concentration of the sample solution (Fuller, 1977). It is expected that this sort of variability will produce scatter, but cannot account for the separation in values between the 0.1g and 0.3g samples.

7.5.2 Scatter of Incident Light

The effects of scatter according to Price (1972) are manifested in two ways. 1. Since some of the incident light is deflected without being absorbed, a spurious increase in the absorption signal is produced. This may lead to considerably higher results than the true one.

2. This spurious absorption assumes that the noise characteristics of the flame and extra noise component are included in the measured signal which, close to the detection limit of the element being measured, may be greater in amplitude than the noise on the true absorption signal.

This effect may be disregarded since blanks of only $HBr + CCl_4 + HNO_3$ were aspirated between each sample solution, and their absorbances read consistently zero for Co and Ni. Therefore, this effect cannot produce the separation between the 0.1g and 0.3g samples.

7.5.3 Memory Effects

Incomplete atomization of an element may cause an enhancement in subsequent analytical determination; if the element is allowed to accumulate in the atomizer the errors become progressively greater (Fuller, 1972). Elwell (1966) states that the rate of vaporization compared with the transit time of the atoms through the flame determines the extent to which the atom is vaporized, and that the most important variables controlling this rate are the boiling point, vapour pressure and atom size. All these factors must be reduced to increase the sensitivity. Therefore, Fuller (1977) states that memory effects are diminished by using higher atomization temperatures or longer atomization time. Price (1972) states that incomplete atomization in a lean flame is not significant.

Memory effects may be eliminated as a cause since,

a) the atomization temperature of 2145 C of the air/acetylene flame is

considered to be high by Reeves and Brooks (1978).

b) The atomization time per sample was 3.0 seconds which is significant to eliminate these effects.

c) The samples ML-81-123 A, B, C, D at 0.3g were analyzed first followed by ML-81-123 E, F, G, H at 0.1g. If memory effects have the potential to create problems then one would expect a gradation from the first samples analyzed at 0.3g to the 0.1g samples. This was not seen, therefore, memory effects are eliminated as a cause for the separation of the two groups.

7.5.4 Condensation

When the atomized element leaves the hot surface of an atomizer it is transported into a much cooler region where condensation of the atomic species can occur. This is enhanced by the presence of large quantities of other elements that are atomized or vaporized at similar temperatures to the element being determined, since the analyte element becomes occluded with the matrix as it condenses (Fuller, 1977). This can be eliminated since no condensation takes place within the atomizing cabinet. Furthermore, it cannot explain the separation between two groups at 0.1g and 0.3g.

7.5.5 Refractory Oxides

Another type of interference shown by Billings (1967) is that certain elements tend to form refractory oxides in the flame.

This may be eliminated since extensive research in the literature could not show either Co or Ni forming refractory oxides.

7.5.6 Ionization Interference

Billings (1967) states that ionization results in a smaller number of the atoms remaining in the ground state sutitable for atomic absorption measurement. If another element is present which can supply free electrons there is an increase in the number of ions returned to the ground state. The result is a positive error or increase in the absorption because of the increase number of ground state atoms. Billings (1965 b) states that the problem can be counteracted by the use of standard additions method.

7.5.7 Spectral Interferences

Spectral interference according to Billings (1967) can occur when using multielement hollow cathode tubes. In these, other elements may emit radiation near the wavelength of the particular element under study.

Spectral interference can be disregarded as a problem since higher concentrations are noted for the Co data of the 0.1g samples as opposed to the 0.3g samples, producing positive error. Therefore, if iron was to be the interfering element, a greater positive error should be expected from the iron-rich solutions. However, this is not the case, as the 0.3g samples appear lower in cobalt than the 0.1g samples.

7.5.8 Molecular Absorption

The difference in the Co values found in the 0.1g and 0.3g samples in Figure 8-1, may be explicable by the formation of molecular species within the air-acetelyene flame that have affected the signal response of the element being determined. The Ni values for both the 0.1g and 0.3g samples have an identical range, thus the behaviour is different from Co.

Hermann and Alkemade (1963) discuss the effects of signal responses of the element being determined, depending on whether it is complexed or present as free atoms. They emphasize that the intensity of the signal is dependent on dissociation, ionization and vaporization processes. Incomplete vaporization of the molecule or chemical changes within the molecule prior to vaporization depend upon the heat of the flame. The flame temperature may be below the dissociation point of such a molecular species and it may be completely vaporized, but even so Hermann and Alkemade (1963) stress that we must consider additional factors, such as the partial pressure of the molecule which may be below its saturation vapour pressure at the temperature of the flame. Price (1972) points out that a stable compound may form within the flame and may depress the signal response, by incomplete molecular dissociation. As a molecular species is aspirated into the flame only part of the metal being determined appears as free atoms, if there is limited dissociation of the complex. Gaydon (1947) lists dissociation energies

of some molecular species, however, he does not include Co-halides, which presumably are present in the solution used. Co-complexes are known to form with all of Br, Cl, NO_3, S under appropriate conditions. Thus one may accept that complexing does occur within the pyrite solution because it contains these ions, although the extent to which they remain in the solution is not known. A part of these ions will have escaped in the form of gas during heating of the solution.

The iron is not the interfering element within the solution since we would expect to see 0.3g samples enriched in Co with respect to the 0.1g samples. However, the Co values of the 0.3g samples are lower than the 0.1g samples and thus the effect of iron can be disregarded.

Interference effects causing these possible complexes have been studied by many workers in a semi-quantitative to qualitative manner. Thus the information on molecular absorption with regards to metals and transition metals is very limited. The extent to which Co-complexing occurs in solution is uncertain. However, we cannot exclude the possibility that there may be stable complexes within the flame. If this is the case, then the formation of complexes might affect the signal of the flame spectrophotometer, producing either an enhancement or a depression in the absorbance readout. In these cases, it would be expected that samples weighed at 0.3g have different complex concentrations than those samples weighed at 0.1g. Thus these

latter samples should approach truer values of Co. It is coincidental that this sample ML-81-123, has the greatest amount of Co, thus it has the greatest amount of error produced as a result of this complexing. Therefore, the errors in the Co values of all other samples are significantly smaller, if we assume it is Co-complexing, however, the accuracy of the analysis still remains unresolved since no external standard could be found. The Ni content does not show similar effects,that is,complexing, although Loftus- Hills and Solomon (1967) cannot convincingly demonstrate, they consider Co complexes more readily than Ni complexes.

Table 7-1

Location	Sample #	Weight (g)	Absorbance					
			Nickel spike (ug/ml)			Cobalt spike (ug/ml)		
			0.0	0.4	0.8	0.0	0.4	0.8
Banded	ML-81-059	0.3005	0.024	0.093	0.168	0.030	0.096	0.166
Sulphide	ML-81-061	0.3006	0.026	0.048	0.120	0.032	0.045	0.149
27th	ML-81-062	0.3004	0.025	0.094	0.169	0.030	0.098	0.166
Level	ML-81-064	0.3007	0.021	0.090	0.170	0.031	0.099	0.168
	ML-81-066	0.3000	0.022	0.091	0.170	0.031	0.097	0.167
Banded	ML-81-048	0.2593	0.018	0.118	0.216	0.037	0.113	0.195
Carbonate	ML-81-049	0.0832	0.005	0.081	0.152	0.012	0.101	0.171
Sulphide	ML-81-050	0.1010	0.005	0.081	0.153	0.020	0.128	0.221
27th	ML-81-051	0.2776	0.035	0.112	0.192	0.052	0.161	0.242
Level	ML-81-052	0.1120	0.005	0.087	0.155	0.014	0.106	0.176
Carbonated	ML-81-043	0.2751	0.011	0.097	0.136	0.010	0.101	0.129
S.F.B.I.F.	ML-81-044	0.3064	0.017	0.116	0.164	0.048	0.106	0.156
	ML-81-046	0.3104	0.013	0.099	0.139	0.037	0.133	0.160
26th	ML-81-079	0.2998	0.013	0.068	0.122	0.033	0.112	0.192
Level	ML-81-080	0.2997	0.013	0.068	0.122	0.033	0.111	0.191
S.F.B.I.F.	ML-81-081	0.2919	0.007	0.085	0.127	0.025	0.137	0.198
	ML-81-082	0.2996	0.006	0.089	0.123	0.033	0.114	0.192
21st	ML-80-953	0.1105	0.008	0.101	0.129	0.013	0.111	0.159
Level	ML-80-954	0.3064	0.034	0.110	0.147	0.096	0.166	0.206
E.S.C.	ML-80-956	0.0801	0.007	0.085	0.127	0.023	0.110	0.152

Table 7-1 continued

Location	Sample #	Weight (g)	Absorbance					
			Nickel spike (ug/ml)			Cobalt spike (ug/ml)		
			0.0	0.4	0.8	0.0	0.4	0.8
24th	ML-80-937	0.0190	0.001	0.025	0.041	0.004	0.043	0.087
Level	ML-80-939	0.2819	0.013	0.096	0.131	0.024	0.106	0.160
E.S.C.	ML-80-942	0.2220	0.014	0.103	0.132	0.013	0.111	0.159
	ML-80-943	0.1817	0.011	0.122	0.154	0.010	0.100	0.137
E.S.C.	ML-80-618	0.2999	0.019	0.100	0.123	0.020	0.121	0.153
30th	ML-80-620	0.0380	0.002	0.082	0.149	0.003	0.118	0.205
Level	ML-80-622	0.0312	0.002	0.084	0.156	0.002	0.116	0.200
Δ3053	ML-80-623	0.0134	0.001	0.047	0.091	0.001	0.044	0.081
	ML-80-870	0.2309	0.075	0.092	0.243	0.022	0.076	0.143
	ML-80-871	0.3008	0.092	0.114	0.261	0.020	0.073	0.140
	ML-80-872	0.3009	0.016	0.150	0.184	0.026	0.117	0.168
	ML-80-873	0.2999	0.015	0.151	0.189	0.019	0.124	0.164
E.S.C.	ML-80-605	0.3011	0.040	0.088	0.168	0.021	0.110	0.145
30th	ML-80-611	0.3012	0.022	0.107	0.148	0.021	0.074	0.141
Level Δ3058								
F-zone	ML-80-986	0.2050	0.008	0.077	0.113	0.032	0.073	0.201
15th	ML-80-987	0.0399	0.003	0.029	0.066	0.009	0.089	0.169
Level	ML-80-991	0.2408	0.010	0.084	0.122	0.001	0.088	0.137
1492	ML-81-001	0.1134	0.005	0.026	0.039	0.015	0.117	0.156
zone	ML-81-002	0.3039	0.079	0.137	0.202	0.072	0.143	0.202
30th	ML-81-003	0.2733	0.037	0.124	0.154	0.039	0.107	0.187
Level	ML-81-004	0.0841	0.011	0.110	0.155	0.016	0.096	0.171

Table7-1 continued

Location	Sample #	Weight (g)	Absorbance					
			Nickel spike (ug/ml)			Cobalt spike (ug/ml)		
			0.0	0.4	0.8	0.0	0.4	0.8
South C	ML-81-124	0.3004	0.016	0.068	0.136	0.057	0.106	0.140
21st	ML-81-125	0.2997	0.005	0.012	0.027	0.007	0.018	0.034
Level	ML-81-126	0.3017	0.009	0.016	0.035	0.005	0.013	0.029
	ML-81-127	0.3006	0.014	0.066	0.135	0.013	0.068	0.136
	ML-81-123A	0.3006	0.029	0.091	0.146	0.110	0.186	0.253
	ML-81-123C	0.3010	0.029	0.089	0.147	0.109	0.187	0.252
	ML-81-123E	0.1001	0.011	0.081	0.145	0.049	0.110	0.170
	ML-81-123F	0.1008	0.011	0.080	0.145	0.045	0.107	0.170
	ML-81-123G	0.1012	0.012	0.081	0.146	0.047	0.109	0.168
	ML-81-123H	0.1014	0.010	0.080	0.144	0.050	0.112	0.170
			0.0	0.1	0.3	0.0	0.1	0.3
	ML-81-123B	0.3006	0.029	0.055	0.081	0.107	0.111	0.119
			0.0	0.5	0.8	0.0	0.5	0.8
	ML-81-123D	0.3011	0.029	0.163	0.286	0.107	0.164	0.232

Table 7-1 (i) Repeated Absorbances

Location	Sample #	Weight (g)	Absorbance	
			Nickel unspiked	Cobalt unspiked
South C 21st Level	ML-81-123A	0.3006	0.029	0.110
	ML-81-123B	0.3006	0.029	0.107
	ML-81-123C	0.3010	0.029	0.109
	ML-81-123D	0.3011	0.029	0.107
	ML-81-123E	0.1001	0.011	0.049
	ML-81-123F	0.1008	0.011	0.045
	ML-81-123G	0.1012	0.012	0.047
	ML-81-123H	0.1014	0.010	0.050

Table 7-2 Determination of x-intercept using Least Squares ($y = mx + b$)
Coefficient of Determination, r^2

Sample #	m	y (y=b)	x (ppm in solution)	r^2	Ni ppm in sample
ML-81-059	0.023	0.018	0.012	0.999	10.630
ML-81-061	0.027	0.018	0.014	0.998	12.325
ML-81-062	0.024	0.018	0.013	0.999	11.096
ML-81-064	0.019	0.018	0.010	0.998	8.555
ML-81-066	0.020	0.018	0.010	0.998	9.159
ML-81-048	0.018	0.024	0.074	0.999	7.139
ML-81-049	0.005	0.018	0.031	0.999	9.539
ML-81-050	0.005	0.018	0.030	0.999	7.577
ML-81-051	0.034	0.019	0.175	0.999	15.828
ML-81-052	0.007	0.018	0.039	0.997	8.730
ML-81-043	0.018	0.015	0.012	0.955	10.951
ML-81-044	0.025	0.018	0.013	0.961	11.322
ML-81-046	0.020	0.015	0.013	0.957	10.568
ML-81-079	0.013	0.013	0.096	0.999	8.057
ML-81-080	0.013	0.013	0.096	0.999	8.058
ML-81-081	0.013	0.015	0.086	0.970	7.421
ML-81-082	0.014	0.014	0.096	0.944	8.081
ML-81-953	0.018	0.015	0.124	0.912	28.158
ML-81-954	0.040	0.014	0.286	0.961	23.394
ML-81-956	0.013	0.015	0.086	0.970	27.029

Table 7-2 continued Determination of x-intercept using Least Squares (y= mx + b)
Coefficient of Determination, r^2

Sample #	m	y (y=b)	x (ppm in solution)	r^2	Ni ppm in sample
ML-80-937	0.002	0.005	0.046	0.986	61.403
ML-80-939	0.021	0.014	0.142	0.947	12.626
ML-80-942	0.024	0.014	0.162	0.920	18.323
ML-80-943	0.024	0.017	0.135	0.907	18.592
ML-80-618	0.028	0.013	0.220	0.906	18.380
ML-80-620	0.004	0.018	0.022	0.997	14.898
ML-80-622	0.003	0.019	0.019	0.998	15.253
ML-80-623	0.001	0.011	0.011	0.999	21.980
ML-80-870	0.052	0.021	0.250	0.825	27.153
ML-80-871	0.070	0.021	0.328	0.844	27.310
ML-80-872	0.032	0.021	0.155	0.894	12.921
ML-80-873	0.031	0.021	0.144	0.904	12.009
ML-80-605	0.034	0.016	0.216	0.979	17.988
ML-80-611	0.029	0.015	0.186	0.960	15.458
ML-80-986	0.013	0.013	0.102	0.968	12.541
ML-80-987	0.001	0.007	0.014	0.989	9.268
ML-80-991	0.016	0.014	0.114	0.966	11.864
ML-81-001	0.006	0.004	0.149	0.981	32.826
ML-81-002	0.077	0.015	0.506	0.998	41.644
ML-81-003	0.046	0.014	0.317	0.926	29.077
ML-81-004	0.020	0.018	0.111	0.955	33.029

Table 7-2 continued Determination of x-intercepty using Least Squares ($y=mx + b$)
Coefficient of Determination, r^2

Sample #	m	y (y=b)	x (ppm in solution)	r^2	Ni ppm in sample
ML-81-124	0.013	0.015	0.088	0.994	7.397
ML-81-125	0.003	0.027	0.133	0.957	11.203
ML-81-126	0.007	0.032	0.215	0.933	17.846
ML-81-127	0.011	0.151	0.073	0.993	6.140
ML-81-123A	0.030	0.146	0.206	0.998	17.154
ML-81-123B	0.032	0.167	0.195	0.964	16.276
ML-81-123C	0.293	0.147	0.198	0.999	16.517
ML-81-123D	0.022	0.315	0.071	0.985	15.909
ML-81-123E	0.012	0.167	0.071	0.999	17.880
ML-81-123F	0.011	0.167	0.069	0.999	17.269
ML-81-123G	0.012	0.167	0.075	0.999	18.673
ML-81-123H	0.011	0.167	0.065	0.999	17.181

Table 7-3 Determination of x-intercept using Least Squares (y=mx + b)
Coefficient of Determination, r^2

Sample #	m	y (y=b)	x (ppm in solution)	r^2	Co ppm in sample
ML-81-059	0.029	0.017	0.172	0.999	14.355
ML-81-061	0.027	0.024	0.112	0.992	9.317
ML-81-062	0.030	0.017	0.176	1.000	14.686
ML-81-064	0.030	0.017	0.180	0.999	14.969
ML-81-066	0.030	0.017	0.178	0.999	14.869
ML-81-048	0.036	0.019	0.182	0.999	17.568
ML-81-049	0.015	0.019	0.076	0.995	22.929
ML-81-050	0.022	0.025	0.089	0.998	22.154
ML-81-051	0.056	0.023	0.238	0.992	21.483
ML-81-052	0.017	0.020	0.087	0.993	19.473
ML-81-043	0.020	0.014	0.137	0.914	12.522
ML-81-044	0.049	0.013	0.365	0.998	29.814
ML-81-046	0.048	0.015	0.315	0.905	25.406
ML-81-079	0.032	0.019	0.165	0.999	13.773
ML-81-080	0.032	0.019	0.165	0.999	13.793
ML-81-081	0.033	0.021	0.154	0.971	13.264
ML-81-082	0.033	0.019	0.168	0.999	14.062
ML-81-953	0.021	0.018	0.116	0.962	26.434
ML-81-954	0.101	0.013	0.073	0.975	59.933
ML-81-956	0.030	0.016	0.189	0.961	58.990

Table 7-3 continued Determination of x-intercept using Least Squares (y=mx + b)
Coefficient of Determination, r^2

Sample #	m	y (y=b)	x (ppm in solution)	r^2	Co ppm in sample
ML-80-937	0.003	0.010	0.030	0.998	40.160
ML-80-939	0.028	0.017	0.168	0.986	14.954
ML-80-942	0.021	0.018	0.116	0.962	13.163
ML-80-943	0.018	0.015	0.118	0.945	16.314
ML-80-618	0.031	0.016	0.189	0.917	15.793
ML-80-620	0.007	0.025	0.030	0.993	19.949
ML-80-622	0.007	0.024	0.028	0.992	22.648
ML-80-623	0.002	0.010	0.020	0.998	37.091
ML-80-870	0.019	0.015	0.131	0.996	14.197
ML-80-871	0.017	0.015	0.117	0.995	9.786
ML-80-872	0.032	0.017	0.184	0.974	15.287
ML-80-873	0.029	0.018	0.164	0.937	13.721
ML-80-605	0.030	0.015	0.1935	0.940	16.069
ML-80-611	0.018	0.015	0.1244	0.995	10.329
ML-80-986	0.017	0.021	0.0828	0.918	10.100
ML-80-987	0.009	0.020	0.0450	1.000	28.153
ML-80-991	0.007	0.017	0.0431	0.974	44.783
ML-81-001	0.025	0.017	0.1446	0.937	31.870
ML-81-002	0.074	0.016	0.4553	0.997	37.461
ML-81-003	0.037	0.018	0.2000	0.997	18.290
ML-81-004	0.016	0.019	0.0868	0.999	25.826

Table 7-3 continued Determination of x-intercept using Least Squares (y=mx + b)
Coefficient of Determination, r^2

Sample #	m	y (y=b)	x (ppm in solution)	r^2	Co ppm in sample
ML-81-124	0.059	0.010	0.573	0.989	47.727
ML-81-125	0.006	0.033	0.182	0.988	15.239
ML-81-126	0.010	0.153	0.122	0.996	10.127
ML-81-127	0.010	0.153	0.070	0.996	5.860
ML-81-123A	0.111	0.178	0.623	0.998	51.875
ML-81-123B	0.107	0.040	0.675	1.000	56.133
ML-81-123C	0.111	0.178	0.621	0.997	51.653
ML-81-123D	0.101	0.151	0.670	0.962	55.644
ML-81-123E	0.075	0.121	0.325	0.999	81.129
ML-81-123F	0.044	0.156	0.286	0.999	71.142
ML-81-123G	0.047	0.151	0.314	0.999	77.550
ML-81-123H	0.050	0.150	0.337	0.999	83.229

Table 7-4 Determination of Error Bars
Standard Deviation and Mean for Sample ML-81-123 A-H

Sample #	Ni (ppm)	Mean	Standard Deviation
ML-81-123 A,B,C,D	65.85833	16.46458	0.52318
ML-81-123 E,F,G,H	71.00545	17.75136	0.68901
Sample #	**Co (ppm)**	**Mean**	**Standard Deviation**
ML-81-123 A,B,C,D	215.3106	53.82699	2.391313
ML-81-123 E,F,G,H	313.0523	78.26307	5.294190

Table 7-5 Percent Particulates Left After Dissolution of Some Py Samples

Sample #	Weight of Sample	Weight of Particulates	Final Sample Weight	Percent Particulates
ML-81-002	0.30390	0.00046	0.30244	0.15
ML-81-043	0.27514	0.00014	0.27500	0.05
ML-81-062	0.30040	0.00035	0.30005	0.11
ML-81-079	0.29984	0.00060	0.29924	0.20
ML-81-080	0.29978	0.00010	0.29968	0.03
ML-81-082	0.29965	0.00014	0.29951	0.04

CHAPTER 8

DISCUSSION OF RESULTS AND PREVIOUS WORK ON Co AND Ni IN PYRITE

8.1 DISCUSSION OF DATA

The analytical results for Co and Ni within pyrite from various localities in the Dickenson Mine are shown in Figure 8-1, and in Tables 7-2 and 7-3. As mentioned in the introduction it is the purpose of this study to determine the source of mineralization in the E.S.C. ore zone. Were the sulphides derived from a) the nearby S.F.B.I.F. or b) from an exotic hydrothermal source whose solution carried its own distinctive suite of trace elements, c) or from some other source. Data from the S.F.B.I.F. and other areas will be discussed in light of the genesis of the E.S.C. ore zone.

Pyrite in the S.F.B.I.F. is thought to precipitate out of sea-water and is characterized by low Co and Ni values. This is shown by the 26th level S.F.B.I.F. (Δ), in Figure 8-1. The 27th level samples of carbonatized S.F.B.I.F. (∇) are enriched in Co except for one sample. Hand specimen examination shows that this sample is unusually low in carbonate in comparison with other samples. This has

also been shown by modal analysis where the results are shown in Table 5-1.

Also from the 27th level pyrite (□) from the banded sulphide unit which is not S.F.B.I.F. but has been interpreted by Lavigne (1983) as remobilized from S.F.B.I.F. (see section 5-1), and impregnated into basalt without the addition of an ore component. The data from this level are identical in Ni and Co to the 26th level S.F.B.I.F. (Figure 8-1), supporting that these sulphides were derived from S.F.B.I.F., The carbonatized S.F.B.I.F. on the 27th level (▽) and the carbonatized banded sulphides from the 27th level (+) have similar Ni contents but contain more Co than unaltered equivalents.

The F-zone (◈) is a sulphide-poor shear zone. Of the three hand specimens examined two of these are carbonate-rich and contain 28 to 44ppm Co and 9 to 11ppm Ni, while the third has very little carbonate and has 10ppm Co and 12ppm Ni. Thus again a positive correlation exists between Co and carbonate.

The South C (●), is a carbonate-quartz vein which shows erratic distribution of Co but uniform Ni values. The high Co values correlates with high carbonate contents. Hand specimen examination of samples ML-81-123 and -124 show massive pyrite blebs in contact with quartz and carbonate. These two samples have the highest Co values, while samples ML-81-125 (pyrite blebs in contact with quartz and carbonate wallrock), ML-81-126 (oxidized pyrite in late quartz fractures) and ML-81-127 (pyrite occurring in blebs and in contact with quartz) are

absent or minor amounts of carbonate are present with lower Co content.

The 21st level E.S.C. and the 1492 shear zones are similar to the F-zone but contain more Ni than the F-zone. These are represented by (■) and (▲) respectively. These samples show higher Ni values with respect to the S.F.B.I.F., and somewhat higher Co. Once again the high Co values corresponds to samples which are carbonate enriched (Table 5-1).

E.S.C. samples from the 24th and 30th levels occupy a field showing similar Co content as the S.F.B.I.F. while the Ni content ranges up to 27 ppm, representing a complete spectrum from the Ni-poor S.F.B.I.F. to Ni-rich epigenetic mineralization such as the 1492 zone and 21st level E.S.C..

It was shown above that the Co content of pyrite is high when it is in contact with carbonate, whether the carbonate be ore-bearing such as E.S.C. or non-auriferous such as carbonatized S.F.B.I.F.. The Co content of the pyrite cannot be used as a discriminator between sedimentary pyrite and those Co values of hydrothermal veins which resemble S.F.B.I.F.. However, Ni values are diagnostic and can be used to discriminate between sedimentary pyrite and hydrothermal pyrite as S.F.B.I.F. is characterized by low constant Ni content and epigenetic pyrite is characterized by higher more variable Ni content. Therefore, it is probable that those pyrite with high Ni content from the E.S.C. ore zone represent hydrothermal sulphides. However, several samples from the E.S.C. ore zone have Ni values similar to S.F.B.I.F. and thus

it is probable that some of the sulphides were derived from the S.F.B.I.F.. This is consistent with the proximity of sulphide-rich E.S.C. ores with the S.F.B.I.F. and that the E.S.C. ore zone cross-cuts the S.F.B.I.F.. Therefore, the data from the E.S.C. can be interpreted to represent a mix between a hydrothermally produced sulphide and that derived from S.F.B.I.F Pyrite from a lens of E.S.C. mineralization on the 21st level which is not spatially associated with S.F.B.I.F. have higher Ni contents. Therefore, it is likely that the sulphides from the E.S.C. ore zone represents a large gold-bearing hydrothermal system which locally intersected a sulphide-rich iron formation whose sulphides were incorporated into the E.S.C. ore zone during metamorphism but have retained their original Co and Ni values.

8.2 COMPARISON OF Co AND Ni CONTENTS IN PYRITE WITH OTHER STUDIED AREAS

The trace element studies presented here have generally pursued one or more of the following criteria as summarized by Loftus-Hills and Solomon (1967): a) determination of temperature of deposition; b) determination of environment of deposition; c) identification of metallogenic provinces; d) proximity of certain types of economic mineralization (Ryall, 1976).

It is my purpose to use available quantitative data to define various depositional environments of pyrite and compare them

LEGEND

△ 26TH LEVEL SULPHIDE FACIES BANDED IRON FORMATION

▽ 27TH LEVEL CARBONATED SULPHIDE FACIES BANDED IRON FORMATION

□ 27TH LEVEL BANDED SULPHIDE

+ 27TH LEVEL BANDED CARBONATE SULPHIDE

◇ 15TH LEVEL F-ZONE

● 21ST LEVEL SOUTH C

■ 21ST LEVEL EAST SOUTH C

▲ 30TH LEVEL 1492 ZONE

⊙ 24TH LEVEL EAST SOUTH C - ARSENOPYRITE

⊖ 24TH LEVEL EAST SOUTH C

C 30TH LEVEL EAST SOUTH C

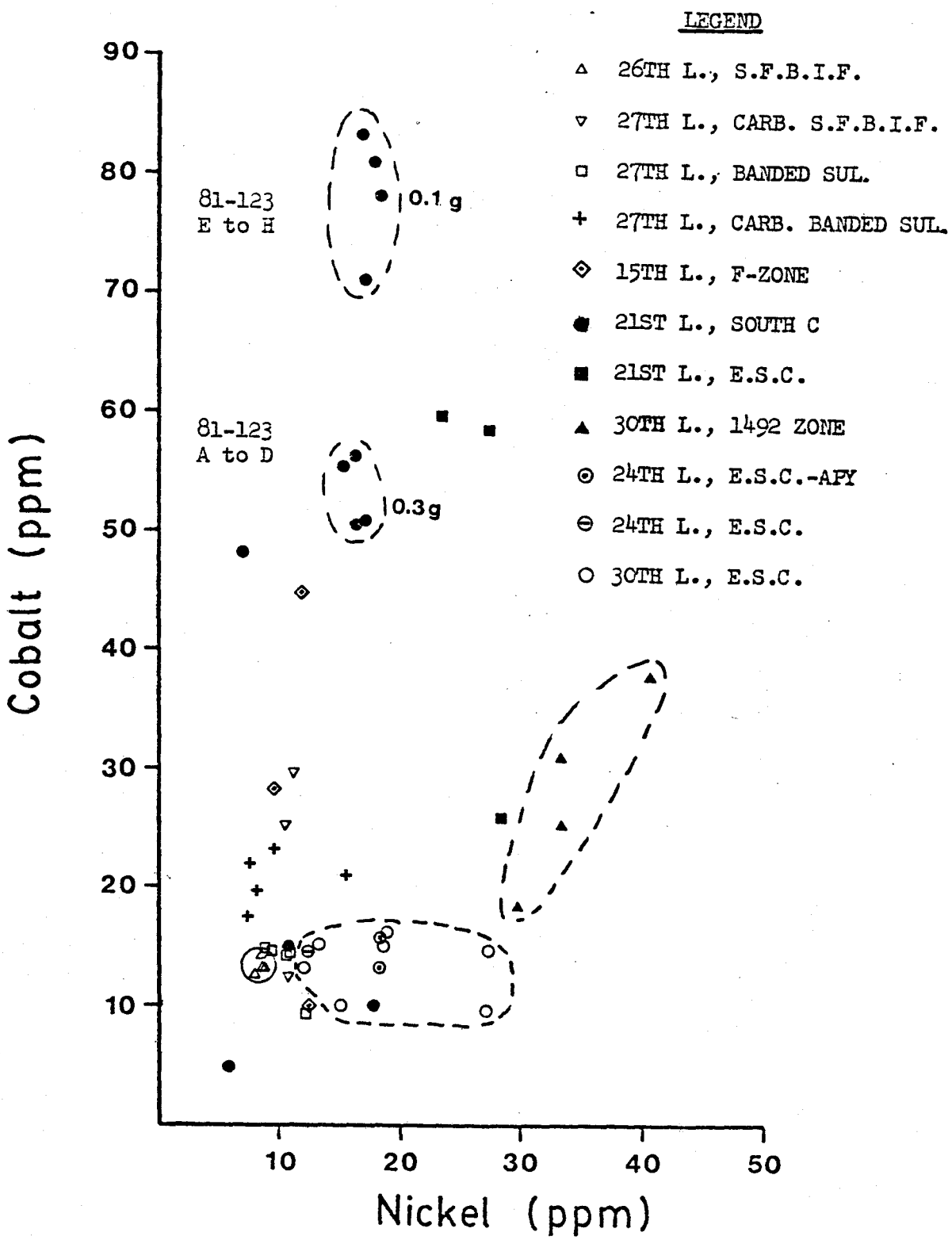
LEGEND
26TH L., S.F.B.I.F.
27TH L., CARB. S.F.B.I.F.
27TH L., BANDED SUL.
27TH L., CARB. BANDED SUL.
15TH L., F-ZONE
21ST L., SOUTH C
21ST L., E.S.C.
30TH L., 1492 ZONE
24TH L., E.S.C.-APY
24TH L., E.S.C.
30TH L., E.S.C.
81-123
E to H
0.1 g
81-123
A to D
0.3g
Cobalt (ppm)
Nickel (ppm)
90
80
70
60
50
40
30
20
10
10
20
30
40
50

FIGURE 8-1

with the new results at the Dickenson Mine. A detailed compilation of the data is presented in Figure 8-2.

Qualitative and semi-quantitative studies have not been included in this compilation, where precision and accuracy were either not mentioned or very poor. These include the following: Mitchell(1968), Hawley (1952), Auger (1940), Fryklund and Harner (1954), Hawley and Nichol (1961), Sutherland (1967), Ryall (1976). Also discarded were those quantitative studies where precision and accuracy were questionable, including Saager and Köppel (1976); Bonatti (1976); Cambel and Kantor (1972).

The various depositional environments outlined in Figure 8-2 are explained in the legend. Hydrothermal exhalative pyrite from massive sulphide deposits overlaps the sedimentary field in Figure 8-2. Plutonic associations such as porphyry Mo-Cu deposits studied by Price (1972) are seen to plot in a smaller field with high Co 60-1600ppm and relatively low 1-100ppm Ni values. Pyrite from various veins overprints the preceding fields showing highly variable Co and Ni. Mokherjee et. al. (1979) have analyzed pyrite from veins of an Archean greenstone belt in India. Their results of the quartz-sulphide lodes are not plotted since they are abnormally high with respect to all other pyrite studies and Co-Ni sulphide contamination may be present.

All of the above studies have used Co/Ni ratios to define environments of ore deposition. However, as can be seen in Figure 8-2 Co/Ni ratios cannot be used, as complete overlap of data from all types of depositional environment exists. As was shown at several localities

at the Dickenson Mine, the Co content of pyrite varies according to the amount of associated carbonate. This most likely reflects changes in fluid chemistry which precipitates the sulphides. As seen in Figure 8-3 the Ni:Co ratios are different for pyrite precipitating from NaF, NaCl, and $NaHCO_3$ solution at various temperatures. Hydrothermal fluids which created gold-deposits also vary in composition. For example Tertiary epithermal gold-mineralization investigated by Casadevall et. al. (1977) found that the ore fluids were water-rich with some dissolved salts. While Guha et. al. (1982) found that an Archean gold depost has fluid inclusions which are pure CO_2.

Thus in order to make use of Co:Ni in pyrite as an indicator of ore genesis we must constrain factors such as fluid composition, temperature of deposition, and most likely the pH, Eh and f_{S_2} by determining the equilibrium mineral assemblage and fluid inclusion studies.

8.3 TEMPERATURE ESTIMATION

The purpose here is to determine a temperature of formation of Dickenson Mine pyrite by comparison with pyrite which has precipiated out of similar solution using Bezmen et. al. (1975) results (Figure 8-3 and Table 8-1).

Without fluid inclusion data on the composition of the fluid in which pyrite precipitated, it is difficult to apply the data by

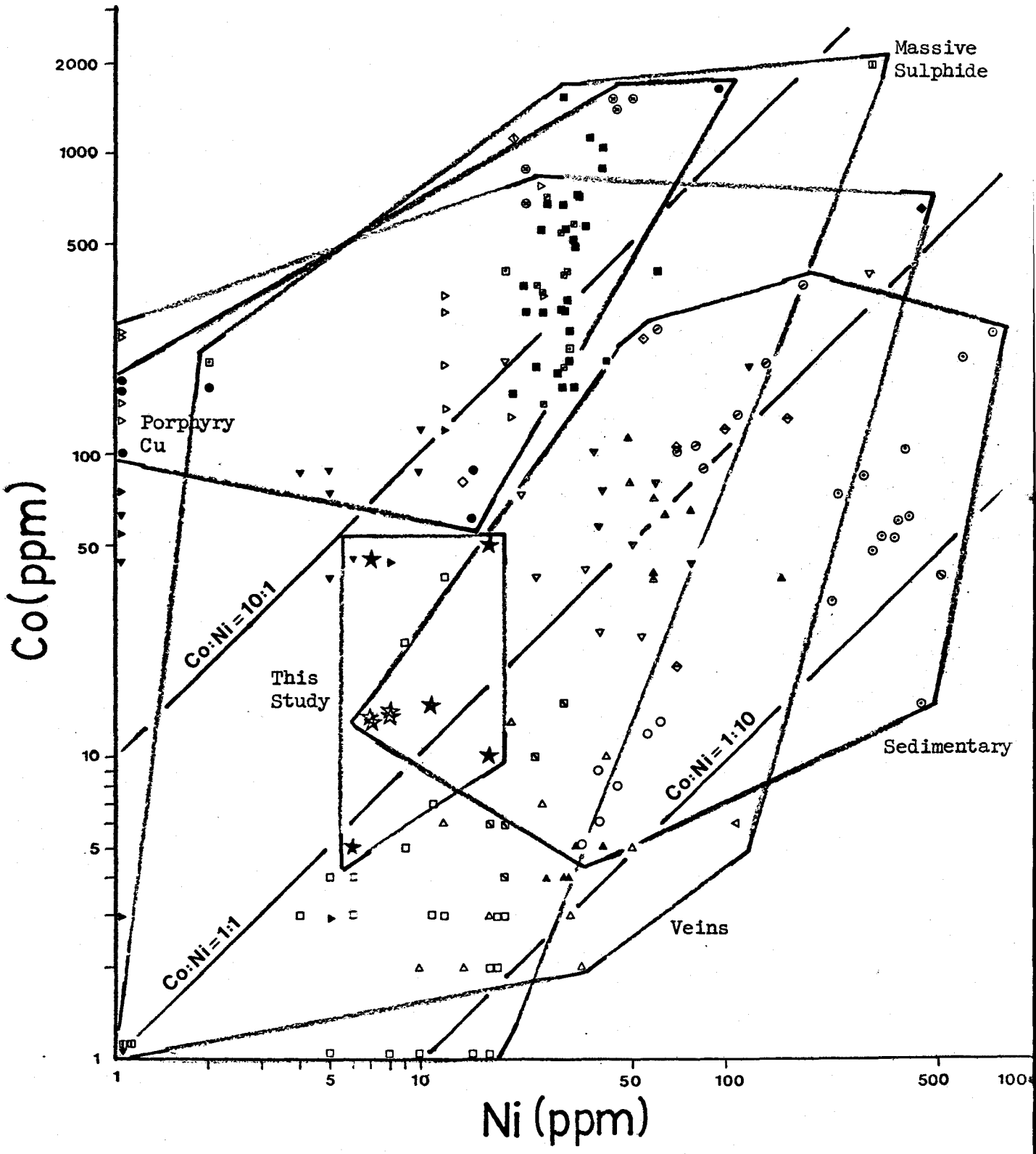

FIGURE 8-2 A compilation of data from several studies.

LEGEND TO FIGURE 8-3

A. SEDIMENTARY PYRITE

- ○ Marine biogenic sedimentary pyrite from carbonate concretions in Lower Jurassic; Yorkshire, England (Raiswell et. al. 1980).
- ⊙ Small nodules and lenses of pyrite in Cambrian banded dark grey slates and shales; Tasmania (Loftus-Hills et. al. 1967).
- ⊘ Fine-grained pyrite in black shales overlying stratiform lodes of pyrite, sphalerite, galena, chalcopyrite that are within volcanics;(Cambrian), Tasmania (Loftus-Hills et. al. 1967).
- ⊘ Pyrite within cherty iron formation afflicted with Cu-rich fluids-from an Archean greenstone belt,India (Mookherjee et. al. 1979).
- ☆ Pyrite from this study of the S.F.B.I.F..From an Archean greenstone belt, Red Lake

B. PYRITE FROM MASSIVE SULPHIDE DEPOSITS

- □ Stratiform lodes of pyrite, sphalerite, galena, chalcopyrite that are within volcanics.(Cambrian),(Loftus-Hills et.al. 1967).
- ▨ Disseminated pyrite in Zn-Pb-Cu deposits in volcanics (Loftus-Hills et. al. 1967).
- ▨ Pyrite lens-shaped bodies associated and interfingered with anhydrite lenses;Paleozoic (Bralia et. al. 1979).
- ■ Massive sulphide bodies very close to quartz monzonite intrusives (Bralia et. al. 1979).
- ▥ Pb-Zn mineralization thought to be stratiform within sediments; Tertiary (Price,1972).
- ⊟ Mineralized pod (chalcopyrite, pyrite, magnetite) replaced propylitized andesites;Tertiary (Price,1972).
- ⊟ Massive sulphide bodies of Cu-Zn, pyrite occur in sheeted vein zones, consisting of numerous lensoid veins;Tertiary (Price,1972).

⋄ Massive sulphide deposits, U.S.S.R. (Branov et. al. 1972).

◈ Massive sulphide deposit, Norway; pyrite from metasediments and metavolcanics. (Gehrisch and Maucher 1975).

◇ Cu-Zn-Pb mineralization in acid volcanic rocks (Silurian) intercalated with sediments; Australia (Roberts , 1981).

◈ Mo mineralization from the Endako molybdenum mine, B.C.; (Dawson et. al. 1974).

C. PYRITE FROM VEINS

△ Pyrite from fissure Pb-Zn-Ag lodes emplaced during orogeny in Cambrian sediments (Loftus-Hills et. al. 1967).

▲ Disseminated pyrite in quartz-veins (veins are within pyrite-chalcopyrite orebody). (Loftus-Hills et. al.1967).

▲ Quartz-cassiterite veins above a granit cupola,(in this area find granites and quartz porphyry of Devonian-Carboniferous age). (Loftus-Hills et. al. 1967).

▽ Pyritic vein ores in quartzmonzonite;Paleozoic (Bralia et. al. 1979).

▼ Pyritic vein ores in allocthonous flysch; Paleozoic (Bralia et. al. 1979).

▼ Pb-Zn-Cu-Au veins within tuffs, and andesites;Tertiary (Price,1972).

▶ Au-Pb-An-Cu veins genetically related to granitic stock in British Columbia;Tertiary (Price,1972).

◁ Zn-Pb-Cu-Au replacement; vein cuts altered andesite-British Columbia;Tertiary (Price, 1972).

▷ Mo mine Pb-Zn-Cu-Ag veins within hornfelsic sediments;(Price,1972).

◆ Pyrite from quartz-carbonate veins;(Price,1972).

★ Pyrite from South C ore zone from the Dickenson Mine.(This study).

D. PYRITE FROM PORPHYRY Cu DEPOSIT

● Mo porphyry deposit ;Tertiary (Price,1972).

⊗ Mo-Cu breccia pipe; Tertiary (Price, 1972).

Bezmen et. al. (1975) to assess the temperature of deposition. If however, we accept that samples ML-81-123, -124, -125, -127, -043, -044 and -046 from the South C and carbonatized S.F.B.I.F. have precipitated from carbonate-rich solutions which were similar in composition to the bicarbonate solution in Figure 8-3 (Bezmen et.al., 1975), then Ni:Co ratios of these samples indicate temperatures of deposition of greater than 500°C. This is consistent with results by Mathieson and Hodgson (in press) who found, on the basis of an arsenopyrite geothermometer and the mineral assemblage of the ore from the Dickenson Mine formed at 500° to 540°C.

8.4 CONCLUSION

Several workers such as Price (1972), Bralia (1979), and Loftus-Hills and Solomon (1967) have attempted to use Co:Ni ratios in pyrite as a means to help define various types of depositional environments. However, as can be seen in Figure 8-2 and according to Loftus-Hills and Solomon (1967) Co:Ni ratios alone are not diagnostic and that concentration levels must also be considered. They further cautioned that in a particular depositional environment the trace elements are likely to have been concentrated under special conditions, and there may be unrecognized provenance factors to take into account.

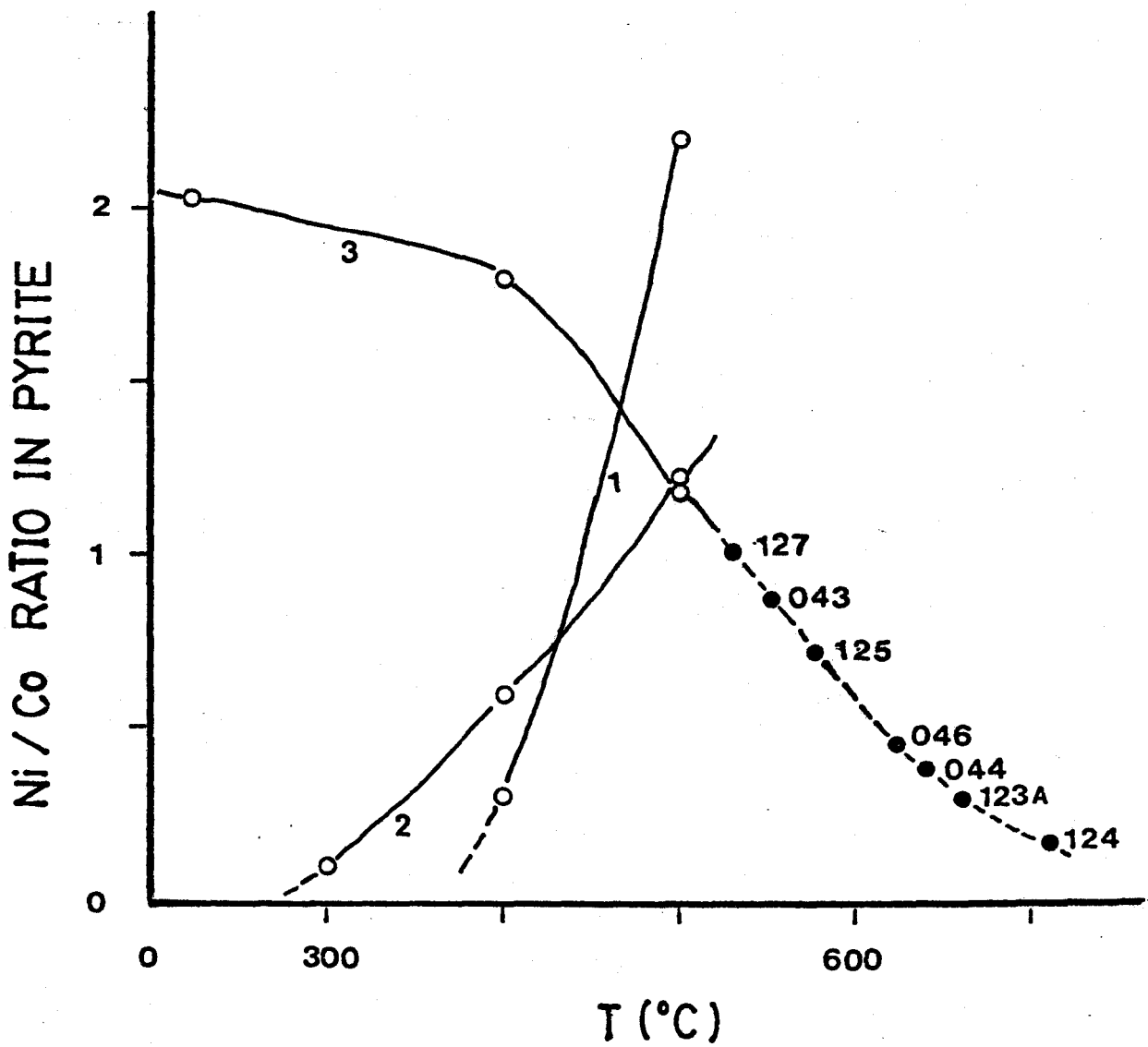

FIGURE 8-3 Effect of temperature on Ni/Co ratio in pyrites synthesized in solution of salts.
1) NaF solution (0.5M); 2) NaCl solution (1 M);
3) $NaHCO_3$ solution (1 M). (From Bezmen et. al. 1975).

TABLE 8-1: Ni:Co Ratios from South C and Carbonatized S.F.B.I.F.. Results plotted in Figure 8-3.

SOUTH C	Ni (ppm)	Co (ppm)	Ni:Co
ML-81-123A	17.154	51.875	0.331
ML-81-124	7.397	47.727	0.155
ML-81-125	11.203	15.239	0.736
ML-81-127	6.140	5.860	1.04

Note: ML-81-126 was not plotted since it is not a representative sample.

CARBONATIZED S.F.B.I.F.			
ML-81-043	10.951	12.522	0.875
ML-81-044	11.322	29.814	0.379
ML-81-046	10.568	25.406	0.415

CHAPTER 9

GENESIS OF THE E.S.C. ORE ZONE AND CONCLUSIONS

9.1 DISCUSSION OF THE ORIGIN OF THE E.S.C. ORE ZONE

In the past few years numerous studies have been made on the E.S.C. ore zone since it represents a major source of gold at the Dickenson Mine. It may represent a syngenetic gold-bearing horizon and is thus the subject of much controversy with respect to its origin. Rigg and Helmstaedt (1980) mapped the ore zone on the 24th level and interpreted it to be dominantly epigenetic, based on structural relationships: however, the arsenopyrite-rich mineralization on the 24th level may represent syngenetic ore (Figure 5-2) as also is the view of Kusmurski (1981). He also interpreted the ore zone on the 30th level as a stratabound felsic volcaniclastic horizon with co-precipitated auriferous volcanic exhalations, based on textural interpretations and assymmetrical geochemical profiles on either side of the ore zone. Kerrich (1981) analyzed samples from the 21-12102 stope (Figure 5-1), and on the basis of oxygen isotope determinations and whole rock geochemistry he concluded that the ore is a mixture of mafic tuff and metamorphogenic hydrothermal solution which exhaled onto the sea floor.

Lavigne and Crocket (1982) express caution on the origin of the ore zone as sulphur isotopes suggest that the sulphur may have been derived from both S.F.B.I.F. and purely epigenetic hydrothermal solutions. Mathieson and Hodgson (in press) examined the arsenopyrite-rich mineralization of the 24th level and considered it to be epigenetic as it replaces mafic volcanic wallrock. The metamorphic assemblage of the ore and an arsenopyrite geothermometer suggest that the ore formed at 500-540 C. Subsequent investigations by Lavigne and Crocket (1983) have found that the ore zone cross-cuts stratigraphy, impregnates basalt and shows a tectonic fabric which developed late in the tectonic history of the volcanic pile. The sulphur isotope ratios suggest that the ore zone was formed by epigenetic hydrothermal fluids, except in the eastern portion where the ore zone intercepts and cross-cuts the S.F.B.I.F. and incorporates its sulphides.

9.2 CONCLUSIONS

The present results may now be discussed in the light of the foregoing. First the Co content of pyrite is not diagnostic as it merely reflects the carbonate content of the solution. The Ni content of pyrite from the E.S.C. ore zone is not suggestive of a syngenetic origin. If the ore zone was a sulphide-rich sediment we should expect that the Ni content of pyrite in both the E.S.C. and the S.F.B.I.F. would be the same since by necessity of their spatial

association they would have to be cogenetic.

The Ni content of pyrite from the E.S.C. falls within the range of that found in the epigenetic mineralization such as the F , 1492 and South C zones, suggesting a similar origin. However, the similarity of the Ni content of a few samples from the E.S.C. to the S.F.B.I.F. suggest that some sulphides in the E.S.C. were derived from the S.F.B.I.F.. This is consistent with the observation of that of the E.S.C. ore zone which cross-cuts the S.F.B.I.F..

In conclusion trace element geochemistry may be used as a means of evaluating ore genesis but strict geological controls are necessary. Finally, each ore deposit studied must be treated uniquely as environmental parameters change from one deposit to the next thus there cannot be a correlation made between any other studies. It is the author's opinion that much work of this type is necessary to understand fully the environmental parameters which control the distribution of trace elements within pyrite.

REFERENCES

Auger, P.E., (1941). "Zoning and district variations of minor elements in pyrite of Canadian gold deposits", Econ. Geol. Vol. 36, 401-423.

Berner, R.A., (1971). Principals of Chemical Sedimentology (ed. McGraw-Hill, New York. 240p.

Bezmen, N.I. and Tikhomirova V.I., (1975). The effect of temperature on distribution of Co and Ni between sulphides and solutions of different composition. Geochem. Intern., 59-64.

Billings, G.K., (1967). Atomic Absorption Sectrometry in Geology. (ed. Angino,E.E.). Elsevier Publ. Co.,London. 144p.

Bither, T.A., Bouchard R.J., Cloud,W.H., Donohue,P.C. and Siemons,W.J., (1968). Transition metal pyrite dichalcogenides high pressure synthesis and correlation of properties. Inorganic Chemistry 7, 2208-2220.

Bonatti, E., Guerstein, M.B.H., Honnorez, J., and Stern, C., (1976). Hydrothermal pyrite concretion from the Romanche Trench (Equatorial Atlantic): Metallogenesis in Oceanic Fracture Zones. Earth and Planet. Sci. Let., 32 , 1-10.

Bralia, A., Sabatini, G., and Troja, F., (1979). A re-evaulation of the Co/Ni ratio in pyrite as geochemical tool in ore genesis problems. Mineralium Deposita, 14, 353-374.

Branov, E.N., Zasukhin G.N., Karpukhina, V.S., Luginova L.A., and Bukharova, V.A., (1972). Occurrence of Cu, Zn, Pb and other elements in pyrite from aureoles of pyrite deposits. Geochem. Intern., 834-844.

Burns, R.G., (1970). Mineralogical Application of Crystalfield Theory. Cambridge Univ. Press. 224p.

Cambel, B., and Kantor, J., (1972). Comparison of isotope and geochemical investigations of sulphides from syngenetic pyrite deposits in the Western Carpathians. In "Recent Contributions to Geochemistry and Analytical Chemistry", (ed. Masior). 424-437.

Casadevall, T., and Ohmoto, H., (1977). Sunnyside Mine, Eureka Mining District, San Juan County, Colorado: Geochemistry of gold and base metal ore deposition in a volcanic environment, Econ. Geol. Vol. 72, 1285-1320.

Dawson, K.M., and Sinclair A.J., (1974). Factor analysis of minor element data for pyrites, Endako Molybdenum Mine, British Columbia, Canada. Econ. Geol. Vol. 69, 404-411.

Elwell, W.T., and Gidley, J.A.F., (1966). Atomic Absorption Spectrophotometry. Second rev. ed. -Oxford: Pergamon Press, 138p.

Fletcher, K., (1970). Some applications of background correction to trace metal analysis of geochemical samples by AAS. Econ. Geol. 65, 588-591.

Fryklund, V.C. and Harner R.S., (1954). Comments on Minor Elements in Pyrrhotite. U.S.G.S., 339-344.

Fuller, C.W., (1977). Electrothermal Atomization for Atomic Absorption Spectrophotometer. Tioxide Intern. Ltd., England. 127p.

Gaydon, A.G., (1947). Dissociation Energies Spectra of Diatomic Molecules. Wiley and Sons Inc. 239p.

Gehrisch, W., and Maucher,A. (1975). Sulphur isotope and trace element analysis from Sulitjelma ore bodies, Northern Norway. Mineral. Deposita 10, 57-59.

Guha, J., Gauthier A., Vallee M., Descarreaux, J. and Lange-Brard, F., (1982). Gold mineralizaion patterns at the Doyon Mine (Silverstack), Bousquet, Quebec. Geology of Canadian Gold Deposits: Proceedings of Symposium, Sept.,1980. Spec. Vol. 24. 286p.

Hawley, J.E., (1952). Spectrographic Studies of Pyrite in Some Eastern Canadian Gold Mines. Econ. Geol. Vol. 47, 260-304.

Hawley, J.E.,and Nichol, I., (1961). Trace elements in pyrite,pyrrhotite and chalcopyrite of different ores. Bull. Soc. Econ. Geol. Vol. 56, 467-487.

Hermann, R., and Alkemade C.T.J., (1963). Chemical Analysis by Flame Photometry. Vol 14. Inter. Publis.,Wiley and Sons, 644p.

Hodgson, C.J., Helmstaedt, H., MacGeehan, P.J. and Rigg, O.M., (1980). Grant 11 Gold ore formation at the Campbell and Dickenson Mines, Red Lake Area. O.G.S. Misc. Paper 93. (ed. Pye). 263p.

Hulliger, F., (1968). Crystal chemistry of chalcogenides and pnictides of the transition elements, Structure and Bonding, Vol. 4,83-229.

Kerrich, R., Fryer, B.J., Milner, K.J. and Pierce, M.G. (1981). The geochemistry of gold-bearing chemical sediments, Dickenson Mine, Red Lake, Ontario: A reconnaissance study. Can. J. Earth Sci. 18, 624-637.

Kusmirski, R.T.M. (1981) Metallogeny of the " East South C " ore zone in the Dickenson Mine, Red Lake, Ontario-Evidence for syngenetic gold deposition. Unpublished M.Sc. thesis, McMaster University. 187p.

Lavigne, M.J. and Crocket, J.H., (1982). A comparative study of sulphur isotope distribution of sulphide facies banded iron formation and East South C ore zone, Dickenson gold mine, Red Lake District; a Preliminary Report. In Current Research, Part A. Geol. Surv. Can. Paper 82-1A, 264-274.

Lavigne, M.J., (1983). Geological, geochemical and sulphur isotopic investigations of gold mineralization and sulphide facies banded iron formation at the Dickenson and Campbell Red Lake Mines, Red Lake, Ontario. Unpublished M.Sc. thesis, McMaster University, Hamilton, Ontario.

Lavigne, M.J., and Crocket, J.H., (1983). Geology of the East South C ore zone, Dickenson Mine, Red Lake. In The Geology of Gold in Ontario. (ed. A.C. Colvine) Ontario Geological Survey, Misc. Paper 110, 141-158.

Loftus-Hills, G. and Solomon, M., (1967). Co, Ni and Se in sulphides as indicators of ore genesis. Mineral. Deposita 2, 228-242.

MacGeehan, P.J. and Hodgson, C.J., (1980). The relationship of gold mineralization to volcanic and alteration features in the area of the Campbell and Dickenson Mines, Red Lake District, Western Ontario. In Genesis of Archean, Volcanic-Hosted Gold Deposits (ed. R.G. Roberts) p. 212-241.

MacLean, W.H., (1976). Sulphides in Leg 37 drill core from the Mid-Atlantic Ridge. G.A.C. Symposium 'Leg 37 of D.S.D.P..

Mathieson, N.A. and Hodgson, C.J., (in press) Alteration, mineralization, and metamorphism in the area of the East South C ore zone, Dickenson Mine, Red Lake, NW Ontario.

Maxwell, J.A., (1968). Rock and Mineral Analysis. (ed. Elving, P.J. and Kolthoff, I.M.) Interscience Publishers, 584p.

Mitchell, R.H., (1968). A semiquantitative study of trace elements in pyrite by spark source Mass Spectrography. Norsk. Geol. Tids. Vol. 48. 65-80.

Mookherjee, A., and Philip R., (1979). Distribution of Cu, Co and Ni in ores and host rocks Inyladhal, Karnataka, India. Mineral. Dep. 14, 33-55.

Nickel, E.H., (1970). The application of ligand-field concepts to an understanding of the structural stabilities and solid-solution limits of sulphides and related minerals. Chem. Geol. 5, 233-241.

Pirie, J., (1980). Regional geological setting of gold-mineralization in the Red Lake area, NW Ontario. In Genesis of Archean, Volcanic-Hosted Gold Deposits. (ed. E.G. Pye and R.G. Roberts). Symposium, Waterloo, Ontario. 387p.

Price, B.G., (1972). Minor elements in pyrites from the Smithers Map area, British Columbia and exploration applications of minor elements studies. Thesis University of British Columbia, 270p, unpublished.

Price, W.J., (1972). Analytical Atomic Absorption Spectrometry. Heyden and Son Ltd., London. 239p.

Raiswell, R., and Plant, J., (1980). The incorporation of trace element into pyrite during diagenesis of black shales, Yorkshire, England. Econ. Geol. Vol. 75, p.684-699.

Ramdohr, P., (1969). The ore minerals and their intergrowths. Intl. Series of Monographs Earth Sciences, Perg. Press Ltd., 1174p.

Reeves, R.D. and Brooks, R.R., (1978). Trace Element Analysis of Geological Materials. Wiley and Sons, Toronto: 421p.

Roberts, I.F., (1982). Trace element chemistry of pyrite: A useful guide for the occurrence of sulphide base metal mineralization. J. Geochem. Expl. 17, 49-62.

Ryall, W.R., (1977). Anomalous trace element in pyrite in the vicinity of mineralized zones at Woodlawn, N.S.W. Australia. J. Geochem. Expl., 8, p.73-83.

Ryall, W.R., (1979). The potential of pyrite-trace element contents to define primary geochemical halos. Publs. Geol. Dep. and Extension Service, Univ. West. Austr. 4, 42 - 59.

Stearns, E.I., (1969). The Practice of Absorption Spectrophotometry. Wiley and Sons:New York. 353p.

Sutherland, J.K., (1967). The chemistry of some New Brunswick pyrites. The Can. Mineral., 71-84.

Volborth, A., (1969). Elemental Analysis in Geochemistry and Geophysics. Elsevier Publishing Co., New York. 373p.

APPENDIX

A. DETERMINATION OF THE AMOUNT OF Ni AND Co SPIKING SOLUTIONS REQUIRED

a) 1 gram Ni (Co) metal powder ÷ 1 litre H_2O =
1,000,000 ug/l = 1000ug/ml

b) 10 ml (pipette) of 1,000 ug/ml + 90ml H_2O =
10,000ug ÷ 100ml = 100 ug/ml (solution used for spike)

c) 0.01 ml = 10 ul micropipette
Take 100 ug/ml (solution) x 4 squirts(0.01 ml) = 4.0 ug
4.0 ug x 10 ul (micropipette) of 100 ug/ml (solution) +
10ml H_2O in volumetric flask + pyrite solution
= 0.4 ug/ml metal + sample
and 0.8 ug/ml metal + sample --spiking solutions used.

B. DETERMINATION OF THE X-INTERCEPT FROM FIGURE 7-3, AND TABLE 8-2 USING LEAST SQUARES ANALYSIS, ALSO THE CORRELATION COEFFICIENT.

A programmable calculator was used to determine the following parameters, of the linear function $y = mx+b$.

The slope $m = \dfrac{\Sigma xy - \dfrac{\Sigma x \Sigma y}{n}}{x^2 - \dfrac{(\Sigma x)^2}{n}}$, where n = number of spiking intervals used.

constant $b = \bar{y} - m\bar{x}$

where $\bar{y} = \frac{\Sigma y}{n}$ and $\bar{x} = \frac{\Sigma x}{n}$;

example: sample ML-81-059

$$\bar{y} = \frac{(0.024 + 0.093 + 0.168)\text{Ni (nm)}}{3}$$

and, $$\bar{x} = \frac{(0.0 + 0.4 + 0.8)\text{Ni (ug/ml)}}{3}$$

from these equations the constant and slope were determined.

C. CORRELATION COEFFICIENT (R^2)

Using the above x and y values and substituting into the following equation:

$$r^2 = \frac{\left(\Sigma xy - \frac{\Sigma x \Sigma y}{n}\right)^2}{\left(\Sigma x^2 - \frac{(\Sigma x)^2}{n}\right)\left(\Sigma y^2 - \frac{(\Sigma y)^2}{n}\right)}$$

D. DETERMINATION OF PPM OF Ni AND Co IN SOLUTION

$$\frac{\text{Concentration of sample} \times \text{25 ml volumetric flask}}{\text{Weight of Sample}} = \text{ppm}$$

example: sample ML-81-059

$$\frac{0.012 \text{ ppm in solution} \times \text{25 ml volumetric flask}}{0.3005\text{g}} = 10.63 \text{ ppmNi}$$

E. DETERMINATION OF PERCENT PARTICULATES LEFT AFTER DISSOLUTION OF SOME PYRITE SAMPLES--TABLE 7-5

(Weight of Particulates ÷ Final Sample Weight) x 100

% particulates left after dissolution of pyrite samples

example: sample ML-81-002

(0.00046 ÷ 0.30244) x 100 = 0.15%